12-19-2013

Investigation of Iron Reduction by Green Tea Polyphenols for Application in Soil Remediation

Jacqueline S. Oakes
University of Connecticut, jacqueline.oakes@uconn.edu

Investigation of Iron Reduction by Green Tea Polyphenols for Application in Soil Remediation

Jacqueline Shannon Oakes

B.S., University of Connecticut, 2011

A Thesis

Submitted in Partial Fulfillment of the

Requirements for the Degree of

Master of Science

At the

University of Connecticut

2014

APPROVAL PAGE

Masters of Science Thesis

Investigation of Iron Reduction by Green Tea Polyphenols for Application in Soil Remediation

Presented by

Jacqueline Shannon Oakes, B.S.

Major Advisor _____
Dr. Marisa Chrysochoou

Associate Advisor _____
Dr. Cristian Schulthess

Associate Advisor _____
Dr. Timothy Vadas

University of Connecticut

2014

ACKNOWLEDGEMENTS

I would like to thank my advisor, Dr. Marisa Chrysochoou, for all of her patience and guidance throughout this degree program and thesis research. Without her academic and personal support I would not have been able to complete this research. I would also like to thank my committee advisors, Dr. CristianSchulthess and Dr. Timothy Vadas, who have also shown great patience and flexibility with my degree schedule. There were also a number of researchers that were not directly related to this project, but were very instrumental in making this research a possibility. I would like to thank: Dr. Jeffrey McCutcheon for the use of his laboratory and equipment as well as his students' help; Heng Zhang from the IMS Surface Science Lab that taught me to use the XPS machine and analyze the data;Dr. M. DarbyDyar from Mount Holyoke College, who ran our samples and analyzed them according to her Mössbauer equipment; and Bruce Ravel from the National Institute of Standards and Technology in New York who allowed us to use his equipment for XANES analysis. I would also like to thank Dr. Chad Johnston who was extremely helpful in the lab and provided useful ideas whenever I was stuck on a problem. Finally, I would like to thank my parents who supported me throughout my entire college education and have allowed me to focus on my education without any outside stressors.

TABLE OF CONTENTS

LIST OF FIGURES

LIST OF TABLES

1. Introduction

1.1 Zero-Valent Iron

Zero-valent iron (ZVI) has been studied and used effectively for many years in groundwater remediation as a chemical reducing agent to degrade toxicants to an innocuous form. Mostl commonly this treatment is performed via a permeable reactive barrier (PRB) (T. Bigg, 2000). In recent years, nanoscale zero-valent iron (nZVI) has been the focus of study as a more effective remediation tool than macroscale zero-valent iron given the same conditions. The nanoscale particles are highly reactive due to their larger surface area, greater number of reactive sites on the particles, and potentially a higher intrinsic reactivity of the reactive surface sites. In comparison with elemental iron, nZVIhas been shown to degrade contaminants such as polychlorinated biphenyls (PCBs) that do not notably react with macroscaleparticles (A. Matlochová, 2013). In many studies, nZVI particles have been shown to degrade contaminants such as trichloroethene (TCE) (M. Otto, 2008) and hexavalent chromium more rapidly and more completely than macroscale ZVI particles (Z. Fang, 2011).

1.2 nZVI Applications

These nZVI particles are growing in popularity as a treatment of groundwater and soils contaminated with chlorinated organic contaminants such as solvents or pesticides, inorganic anions, heavy metals (N. Mueller, 2012), PCBs, nitrates, and even uranium (A. Matlochová, 2013). Cr(VI) could be rapidly reduced and immobilized by nanoscale iron-based particles by reduction and generation of Cr(III), which is then coprecipitated with Fe^{3+} on the surface of the nanoparticles (B. A. Manning, 2007). Another major advantage of nZVI over macroscale ZVI is that it can be directly injected into the aquifer using infiltration wells, a sleeve pipe, push

infiltration, or gravity infiltration, which results in faster and more effective groundwater remediation than traditional pump-and-treat methods or PRBs (N. Mueller, 2012).

There are some challenges in using nZVI as a remedation tool in the field such as iron passivation through non-target reactions, limited particle mobility due to agglomeration, and the difficulty of scaling up laboratory methods for field application (N. Müller, 2010). There is also an uncertainty as to the long-term environmental effects posed by using nZVI*in situ* as this is a relatively recenttechnology. While nZVI is generally considered an appropriate remediation tool, actual evaluations of persistence, bioaccumulation, toxicity, and other criteria for environmental concern are mostly unknown due to a lack of suitable data (K. D. Grieger, 2010).

These concerns keep the research community invested in improving this suspension as a tool and continuing to optimize its properties and observe its secondary effects. Many recent studies have investigated combining nZVI with organic material. Mixing nZVI with organic matter has shown to increase reactivity, accelerate reduction, and improve the physical structure of the Fe^0 (J.X. Liu, 2009). Some have suggested that organic matter may be able to synthesizenZVI in a single step without harmful byproducts (G. E. Hoag, 2009). The following research will focus on studying this particular claim in order to better understand the reaction between organic matter and iron. The source of organic matter for this study will be green tea polyphenols as these have been shown to synthesis nZVI and stabilize the nZVI particles to prevent agglomeration (M. N. Nadagouda, 2009). This study will investigate these claims by characterizing the full suspension, liquid solution, and solid precipitate of various mixtures of iron and green tea.

2. Literature Review

2.1 Synthesis Methods for NanoscaleZero-valent Iron

There are several accepted methods of synthesizing nZVI particles. Almost all methods fall under two categories. One category starts with a larger microscale or granular product and then generates nanoparticles through a mechanical or chemical breakdown such as milling, etching, sputtering, or machining. The other approach creates nanoparticles structures by building them through chemical synthesis or some self-assembling process (X-Q. Li, 2006). Some common practices include: preparing nanoparticles in aqueous solutions by using sodium borohydride to reduce ferric or ferrous iron (R. Yuvakkumar, 2011); decomposing pentacarbonylat elevated temperatures in organic solvents to produce zero-valent iron (D. L. Huber, 2005); or synthesis from hydrogen reduction of iron oxides such as goethite or hematite at elevated temperatures (X-Q. Li, 2006). The simplest and most common of these methods used in research is reduction via sodium borohydride according to the following reaction:

$$4Fe^{3+} + 3BH^{-}_{4} + 9H_2O \rightarrow 4Fe^{0}_{(precipitate)} + 3H_2BO^{-}_{3} + 12H^{+} + 6H_{2(gas)}$$

The basic lab setup of this synthesis involves slowly titrating a 0.2M solution of $NaBH_4$ into a constantly mixing solution of 0.05M $FeCl_3 \bullet 6H_2O$ in a 3-neck flask reactor until a 1:1 ratio has been achieved. The generated iron nanoparticles are then harvested either through vacuum filtration or repeated centrifugation (Y-P. Sun, 2006). This procedure is easily performed, however it does have safety concerns. The synthesis needs to be performed in a fume hood to collect the hydrogen gas byproduct and explosion-resistant mixers need to be utilized to prevent the possibility of sparks (X-Q. Li, 2006).

It is common practice to prevent aggregation of metallic nanoparticles by a stabilizer such as a soluble polymer or surfactant. This stabilizer can either be added before aggregates have formed, or can be added after agglomerations have been mechanically broken apart. These

stabilizers provide inter-particle electrostatic and steric repulsions that outweigh the inherent Van der Waals and magnetic attractive forces that cause the particles to agglomerate (M.N. Nadagouda, 2009). nZVI particles usually exhibit a core-shell structure with zero-valent iron surrounded by a mixed valent (Fe^{2+} and Fe^{3+}) oxide shell. There are many stabilizers that can be chosen from to effectively inhibit agglomeration and oxidation of the iron cores of these nanoparticles. Some organic examples include polyethylene glycol (PEG), methoxyethoxyethoxyacetic acid (MEEA), and polyacrylic acid (B. Kharisov, 2012).

A single-step synthesis of nanoscalezero-valent iron was first proposed by Nadagouda et al. (2009) and Hoag et al. (2009). They suggested that the caffeine and polyphenols found in green tea can act as both reducing agents for nZVI synthesis and as stabilizing agents by capping nanoparticles before they can agglomerate. Tea extract was chosen because it is biodegradable and water soluble at room temperature. Tea extract of 20 g/L was reacted with 0.1N $Fe(NO_3)_3$ at room temperature in different compositions ranging from 10ml tea extract + 1mL 0.1N $Fe(NO_3)_3$ to 1mL tea extract + 10mL 0.1N $Fe(NO_3)_3$ as detailed in Table 2.1.

Table 2.1.1: Preparation of nanoscalezero-valent iron particles using tea (M.N. Nadagouda, 2009)

Sample ID	Composition Description
T1	10 mL tea extract + 1 mL 0.1 N $Fe(NO_3)_3$ solution
T2	5 mL tea extract + 5 mL 0.1 N $Fe(NO_3)_3$ solution
T3	1 mL tea extract + 5 mL 0.1 N $Fe(NO_3)_3$ solution
T4	1 mL tea extract + 10 mL 0.1 N $Fe(NO_3)_3$ solution
T5	5 mL tea extract + 4 mL 0.1 N $Fe(NO_3)_3$ solution
T6	5 mL epicatechin (0.01 N) extract + 1 mL 0.1 N $Fe(NO_3)_3$ solution
T7	4 mL epicatechin (0.01 N) extract + 4 mL 0.1 N $Fe(NO_3)_3$ solution
T8	5 mL tea extract + 2 mL 0.1 N $Fe(NO_3)_3$ solution
C1	(Control) 2 mL $Fe(NO_3)_3$ + 10 mL $NaBH_4$
C2	(Control) 1 mL $Fe(NO_3)_3$ + 10 mL $NaBH_4$
C3	(Control) 1 mL $Fe(NO_3)_3$ + 5 mL $NaBH_4$

Nadagouda et al. (2009) postulated that iron nanoparticles formed upon mixing of these two solutions by caffeine and polyphenols complexing and simultaneously reducing Fe^{3+} to

$Fe^0$and then capping the resulting nanoparticles. Characterization of the resulting particles formed during reaction was performed with comparative transmission electron microscopy (TEM), UV-Vis spectra, and XRD analyses. The reduction of iron was supported by comparing the UV spectra of tea extract, $Fe(NO_3)_3$, and of the mixture, with the reacted mixture having broad spectrum absorption at higher wavelengths and no sharp absorption at lower wavelengths as in either of the controls. X-ray diffraction was also performed to confirm phase formation. Nadagouda et al. (2009) found two compositions (T3 and T4) to be amorphous. Two other compositions (T1 and T8) had very small peaks that could be indicative of hexagonal Fe. Only one composition (T2) had an XRD scan showing a distinct peak that could be indexed to Fe_2O_3. The TEM scans showed a wide range of nanoparticle size, shape and structure depending on the concentration of tea extract (M. N. Nadagouda, 2009).

Similarly, Hoag et al. (2009) reacted 20 g/L of filtered green tea (GT) with 0.1M $FeCl_3$ salt in a 2Fe:1GT composition ratio to form a 66mM Fe solution. This synthesized GT-nZVI was then studied as a tool to degrade bromothymol blue (a model contaminant) in the presence of H_2O_2(a bromothymol blue stabilizer) compared to two commonly used iron chelates: Fe-ethylenediaminetetraacetate (Fe-EDTA) and Fe-(S,S)-ethylenediamine-N, N'–disuccinic acid (Fe-EDDS). The GT-nZVI was found to be a better catalyst than the Fe-EDTA and Fe-EDDS for free-radical production from H_2O_2due to the presence of zero-valent iron in this mixture.

2.2 Green tea polyphenols properties and reaction with Fe

Polyphenols have been studied in great depth in food chemistry and biochemistry. They are noted as important antioxidants and have been measured in various types of food. Foods and beverages especially high in antioxidants in the form of polyphenols include tea, coffee, and red

wine. These polyphenols interfere with iron absorption, reducing the bioavailability of iron and can lead to an iron deficiency (R. I. Mellican, 2001).

The Folin-Ciocalteu colorimetricassay performed on various brands of commercially available green tea yielded a range of 14-22 gallic acid equivalents (GAE) (in g/100g of plant material) of total polyphenols (C. Anesini, 2008). Green tea, on average, has a higher polyphenol content than black tea due to the further oxidation of black tea in a post-maturation process of fermentation, which does not occur in green tea, because it is steamed prior to drying and this inactivates the enzymes that cause oxidation (P. Ryan, 2007). The higher polyphenol content directly relates to a higher antioxidant capacity (C. Anesini, 2008).

There are many different groups of polyphenols found in green tea and these different groups have been quantified using High Performance Liquid Chromatography (HPLC) and other methods. The functional groups with the most biological benefits are flavanols. Four flavanol derivatives are found in tea, shown in Figure 2.1: epicatechin (EC), epigallocatechin (EGC), epicatechingallate (ECG), and epigallocatechingallate (EGCG). These account for 9-13% of the overall dry weight of the tea (Ryan, 2007).

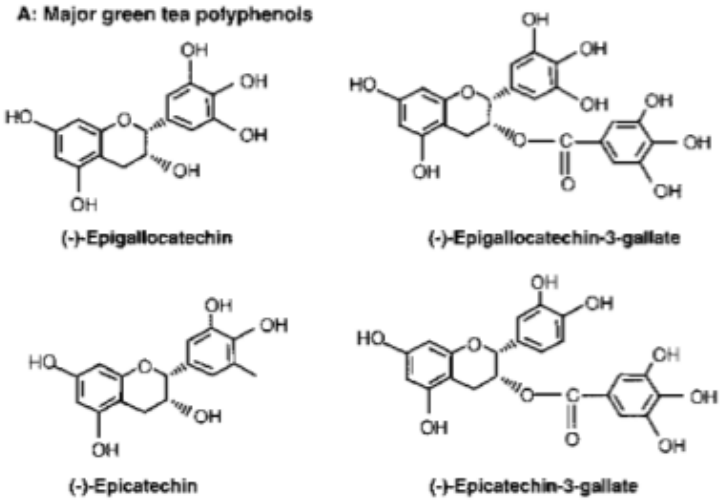

Figure 2.2.1 The four major flavanol structures found in green tea (C. Anesini, 2008)

Henning et al. (2003) measured the concentrations of different polyphenols in various green tea solutions from different brands; representative results are shown in Table 2.2.1. The results indicate that thecompounds EGCG and EGC are approximately 66% of the total dissolved mass of polyphenols in green tea, or 56% on a molar basis.

Table 2.2.1: Concentrations of polyphenol compounds in various green tea brands (from Henning et al., 2003)

	MW (g/mol)	Concentration (mg/100 mL)			Average mass fraction (%)	Average molar fraction (%)
		Bigelow	Celestial	Uncle Lee		
Gallic acid	170	1.5	0.6	1	0.7%	1.3%
Caffeine	194	23.6	33.6	29.4	16.7%	27.5%
EGC	306	30.9	79.7	49.2	28.6%	30.0%
Catechin	290	0	4.4	3.6	1.2%	1.4%
Epicatechin	290	6.5	13.3	15.4	6.5%	7.1%
EGCG	458	42.5	99.3	65	37.4%	26.2%
GCG	458	4.1	5.4	4.3	2.7%	1.9%
ECG	442	3.6	4	15.9	4.4%	3.2%
Catechingallate	442	0	10	2.4	1.8%	1.3%

There are no detailed reports in the literature with regard to the reduction of Fe(III) to Fe(0) by polyphenols, even though older studies indicated that polyphenol-rich foods could react with Fe to change the properties of Fe absorption and of the food color (R. I. Mellican, 2001). Viteri et al. (1995) reported that tea turned black when Fe-fortified sugar was added, which is probably the first report of the production of iron nanoparticles from green tea. However, there are several studies that document the reduction of Fe(III) to Fe(II) by polyphenols, in conjunction with iron absorption studies from food and the anti-oxidant role of polyphenols (R. I. Mellican 2001, Perron and Brumaghim 2009 and references therein). In an attempt to understand the color change in various foods that reacted with iron salts, Mellican (2001) mixedferric sulfate and ferrous sulfate mixed with catechols and assessed the production of Fe(II) using a ferrozine assay. The results suggested that the reactive iron species was ferric and that the black color

development was indicative of its reduction to the ferrous state. It was also suggested that ferrous iron in the presence of catechols would first oxidize to ferric iron and then slowly develop color as the ferric iron then reduced back to ferrous iron (R. I. Mellican, 2001).

The reaction between specific polyphenol compounds and ferric iron was studied in detail by Hynes and Coinceanainn (2001) and Ryan and Hynes (2007) for low and high MW polyphenols, respectively. The proposed reaction pathways in these two studies are shown in Figure 2.2.2.

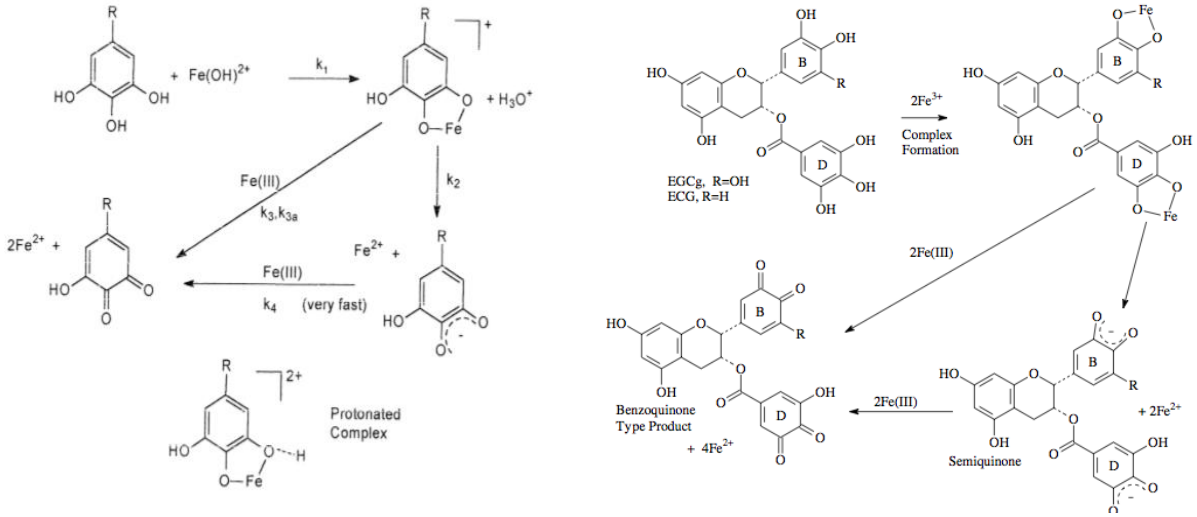

Figure 2.2.2: Reaction pathway of catechin with Fe(III) (left, from Hynes and Coinceanainn 2001) and EGCG with Fe(III) (right, from Ryan and Hynes 2007)

This reaction of both low MW catechin and EGCG with ferric iron occurs in two main steps, one involving complex formation and the second an electron transfer reaction. In this second step, the ferric iron is reduced to ferrous iron and the catechin is oxidized to the corresponding quinone either directly or through the production of a secondary semi-quinone (Hynes and Coinceanainn, 2001). Figure 2.2.2 indicates that low MW quinones can only bind one Fe^{3+} atom in the first step and produce up to 2 Fe^{2+} atoms per reaction, while EGCG and high MW compounds can produce complexes with 2 Fe atoms and produce up to 4 atoms of Fe^{2+} per reaction. However, the amount of Fe produced also depends on the Fe:polyphenol ratio. A

1:1 molar ratio can only produce 1 mol of Fe^{2+} per mol of polyphenol regardless of the MW, while a 4:1 ratio can produce the full 4 mols of Fe^{2+} per mol of high MW polyphenol.

Overall, Fe^{3+} will be reduced by many different components found in tea and modeling of this reduction is usually simplified by using the most prolific reduction ratio as representative of the whole reaction (Hynes and Coinceanainn, 2001). However, in reality it is the addition of these separate reactions that each work to reduce Fe^{3+}.

The following study will focus on how these polyphenols affect Fe reduction at specific concentration ratios to determine the valency and speciation of Fe in suspension. Then these concentration ratios will be tested for efficiency as a remediation tool.

3. Methods

3.1 Preparation of Green Tea-Iron Suspension

The green tea-iron suspension was prepared based on the method proposed in Hoag 2009. Chunmee Special Grade #1 green tea leaves from Imperial Tea Garden were used in all experiments. The tea was brewed at 80^{o}C for 30 minutes. The leaves were then vacuum filtered using a Millipore prefilter (> 5 μm). The resulting filtrate was then vacuum filtered using a Millipore Durapore sterile, plain, white filter with a pore size of 0.22 μm. This solution was prepared fresh daily and stored at 4^{o}C throughout the day. The 0.1M Fe solution was prepared using ferric chloride hexahydrate. These two solutions were mixed together at room temperature at composition ratios of 2Fe:1GT to form 66mM Fe, 1Fe:2GT to form 33mM Fe, and 1Fe:5GT to form 16.7mM Fe.

Total polyphenol content of the 3 suspensions and of the green tea solution at various brewing times and tea concentration was measured using a modified Folin-Ciocalteu assay as

described in International Organization for Standardization (ISO) 14502-1. A 1000 μg/mL gallic acid stock solution was prepared fresh daily by dissolving 110 mg of gallic acid monohydrate in 100mL DI water. Green tea solution was centrifuged at 3500rpm for 10 minutes and diluted 1:100 for sample testing. A 5mL of Folin-Ciocalteu phenol reagent from Sigma-Aldrich (catalog number 47641) was reacted with 1mL of green tea and 4mL of 7.5% (by mass) sodium carbonate solution for 1 hour. The absorbance was measured at 765 nm. The polyphenol concentration was calculated according to the following equation:

$$[P] = ((D_{sample} - D_{intercept}) * d) / m$$

Where [P] = polyphenol content expressed in μg/L gallic acid equivalents (GAE)
D_{sample} = optical density of sample test solution
$D_{intercept}$ = optical density at the point the best-fit linear calibration line intercepts the y-axis
d= dilution factor
m= slope of calibration curve

3.2 Sample Fraction Analysis

The samples were analyzed according to the schematic in Figure 3.2.1 below:

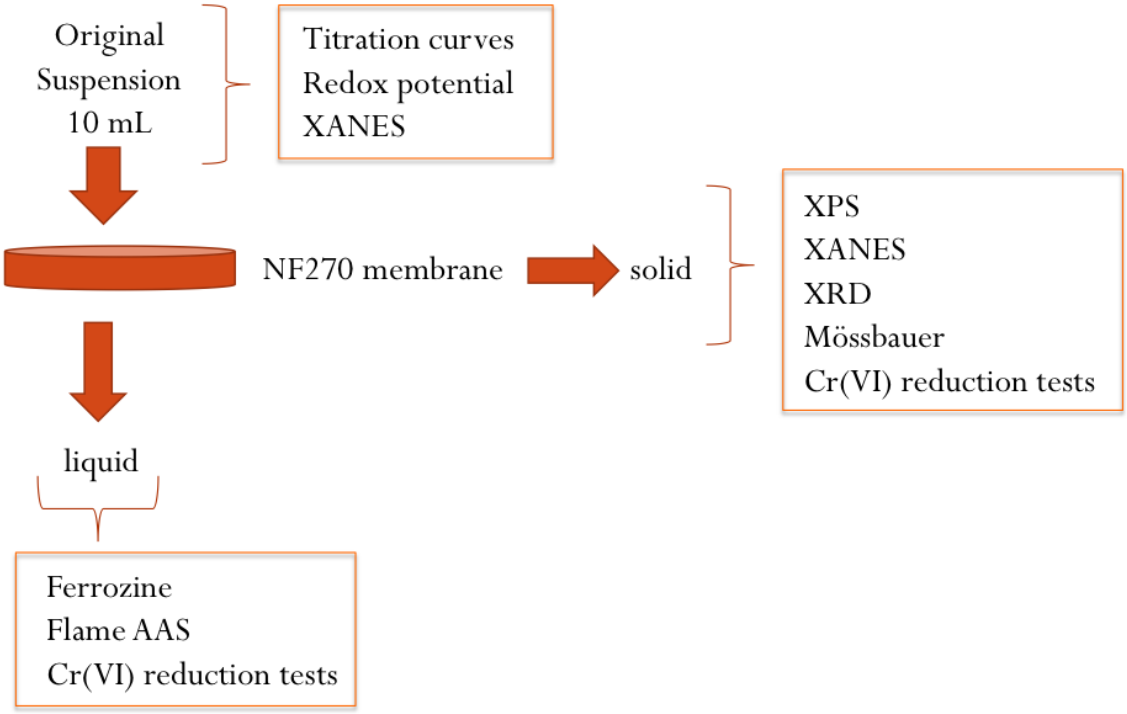

Figure 3.2.1 Breakdown of Methods Used for Analysis on Each Fraction of Total sample

Most of the methods used were not capable of giving results on the sample in suspension, except for the X-Ray Absorbance Near Edge Spectroscopy (XANES). Thus, the suspension was separated into a solid and a liquid fraction through filtration or centrifugation.

The solid was tested using X-Ray Photoelectron Spectroscopy (XPS), XANES, X-Ray Diffraction (XRD), Mössbauer Spectroscopy, and Cr(VI) reduction capacity tests, which are all described in detail in the following solid analysis section. These spectroscopy methods have all been shown to identify iron valency and speciation in previous studies.

The liquid was analyzed using the Ferrozine Assay to determine Fe2+ concentration and Flame Atomic Absorption Spectroscopy to determine total Fe concentration. The reduction tests were performed to analyze the respective importance of each fraction in remediation.

3.3 Suspension Analysis

3.3.1 Titration curves

A small amount (10-20mL depending on ratio of green tea to iron) of constantly stirring GT-Fe suspension was titrated using 0.25M NaOH over the pH range of 2-12. The NaOH was added in discrete amounts according to the buffering capacity of the suspension. The pH was allowed to stabilize before a reading was recorded and more NaOH added. Titrations were also modeled with Visual MINTEQ software for various Fe concentrations.

3.3.2 Redox Potential

An InLabMettler Toledo Ag Redox electrode was used to read oxidation reduction potential for each suspension and green tea solution.

3.3.3 X-Ray Absorption Near Edge Spectroscopy Analysis on Iron in Suspension

XANES analysis was performed on beamline X23A2 operated by the National Institute of Standards and Technology, at the National Synchrotron Light Source (Brookhaven National Laboratory, Upton, NY). Incident X-ray energy was scanned across the XANES region (100 eV below the edge up to 400 eV above the edge) of the Fe K-edge (E= 7112 eV) using a Si(311) monochromator and a single-bounce harmonic rejection mirror. The monochromator was calibrated using an Fe foil. Fluorescent X-rays were collected using a Stern-Heald fluorescence detector. Samples of the GT-nZVI suspensions were pipetted into a sample holder between two layers of Kapton tape for analysis. Final spectra are the result of three averaged scans. XANES data were processed using the Athena software (Ravel and Newville 2005), including normalization, calibration and alignment.

3.4 Separation of Liquid and Solid Fractions

The solid fraction was separated from the liquid fraction through nanofiltration in custom built stainless steel dead end cells. The cells have a 33.2 cm^2 membrane area. NF270 filter paper (pore size ~ 1 nm) from Dow Water & Process Solutions was cut to fit the cell diameter using an X-ACTO knife and rinsed with DI water before being fit into the cell. A 10mL aliquot of sample was pipetted into the cell for each test. Nitrogen from a high-pressure tank flowed into the cell at 500psi. The cell was positioned atop a stir plate and the outflow was captured in a plastic screw-cap vial. The filtration ran to completion. The filtrate was stored at 4^oC. The filter paper and solid mass were transported in petri dishes to a desiccator with continuous flow of nitrogen gas until dried. They were then wrapped in parafilm and stored in a vacuum-sealed plastic bag at 4^oC. The nitrogen flushing of the samples was done to prevent oxidation.

3.5 Liquid Fraction Analysis

3.5.1 Fe^{2+} Concentration Through Spectroscopy

Fe^{2+} concentration was determined using a revised Ferrozine method (Viollier, 2000). This updated methodology was used to avoid boiling the sample and potentially damaging organics. All chemicals used were ACS reagent grade. A 10^{-2} Mferrozine solution was made by dissolving 3-2(2-Pyridyl)-5, 6-diphenyl-1, 2, 4-triazine-p, p'-disulfonic acid monosodium salt hydrate (Sigma-Aldrich) in 0.1M ammonium acetate solution. The reducing agent was a 1.4M hydroxylamine hydrochloride solution dissolved in 2M hydrochloric acid. The buffering agent was a 10M ammonium acetate solution, adjusted to pH 9.5 with ammonium hydroxide (28-30 wt% NH_3 solution). Standards were prepared from a 1 mg/L Fe^{3+} stock solution in 10^{-2}M HCl.

Filtrate from the dead end nanofiltration was diluted in a 1:1000 ratio immediately

afterfiltration to minimize possible iron transformation and the assay was performed on the same day. A 2.5mL aliquot of sample was pipetted into a plastic cuvette. A 250 µLaliquot of ferrozine solution was added to the cuvette and gently shaken to evenly distribute the color development. The absorbance was read at 562nm and recorded. A 375 µLaliquot of reducing agent was pipetted into the cuvette and gently shaken to mix. The cuvette stood for 10 minutes before 125 µL of sodium acetate buffer solution was pipetted into the cuvette. The cuvette was shaken and the absorbance recorded. For the calibration standards, an additional 500 µL of DI water was pipetted into the cuvette and absorbance was recorded for use in the dilution factor, alpha. The Fe^{2+} concentration was determined according to the equation:

$$C_{Fe(II)} = \frac{A_1 \varepsilon_{Fe(II)} l\alpha - A_2 \varepsilon_{Fe(III)} l}{\varepsilon_{Fe(II)} l\alpha(\varepsilon_{Fe(II)} l - \varepsilon_{Fe(III)} l)}$$

Where:
A_1 = Measured absorbance before reduction step
A_2 = Measured absorbance after reduction step
$\varepsilon_{Fe(III)}l$ = Slope of A_1 calibration curve
$\varepsilon_{Fe(II)}l\alpha$ = Slope of A_2 calibration curve
α = Dilution factor

3.5.2 Flame Atomic Absorbance Spectroscopy

The filtrate was measured at a dilution ratio of 1:100 and was acidified when needed using HNO_3. Standards were taken from a 1g/L Fe^{3+} in HCl stock solution.The total iron concentration of the filtrate was determined using EPA method 236.1 for FlAAS.

3.5.3 Cr(VI) Reduction by Liquid Fraction

A stock solution of 50 mg/L as Cr(VI) was prepared using potassium dichromate. A

5mLaliquot of the filtrate was separated and 25mL of the 50 mg/L as Cr(VI) solution was added to it. The solution was mixed and the pH was measured. Drops of HNO_3 were added to lower the pH to a value between 2 and 4 if necessary. The solution was then allowed to react overnight. The solution was diluted 1:10 with DI water and the Cr(VI) concentration was measured using colorimetric EPA Method 7196a.

3.6 Solid Fraction Analysis

3.6.1 X-Ray Photoelectron Spectroscopy Analysis

Sections from the dried filter post nanofiltration were cut and mounted on carbon tape the sample holder. The XPS operates under nitrogen rich conditions and scans are run once oxygen has been depleted from the system. The XPS scan was carried out using a PHI Multiprobe with an aluminum anode. The full survey spectra were collected using a pass energy of 100 eV and a scan rate of 1eV per step. A full survey spectrum was collected for each sample. High resolution spectra were collected for each sample over the carbon peak and over the range where iron peaks appear. The high resolution spectra were collected at a pass energy of 50 eV and a scan rate of 0.1 eV per step. High resolution scans were performed on other prominent peaks if relevant such as oxygen. Iron species bound to oxygen would appear in the iron peaks and in the oxygen peaks. The spectra were analyzed using CasaXPS software. Binding energy data was derived from the spectra fitting. All spectra peaks were calibrated to the graphite peak shift of the full survey for each sample.

3.6.2 X-Ray Absorption Near Edge Spectroscopy Analysis

XANES analysis on the filtered solids was performed according to the same method as the suspension described in section 4.2.3.

3.6.3 Mössbauer Spectroscopy Analysis

Mössbauer spectra (MS) were recorded using a conventional spectrometer of constant acceleration with a 57Co(Rh) source of 10 mCi. A closed-cycle cryostat (CCS 850 Janis) was employed for low temperature measurements. The Mössbauer data were evaluated with the Recoil software (University of Ottawa, Canada) using a Lorentzian-based spectral fitting routine for the doublets and Voigt base fitting for broadened sextets. All isomer shifts given referred to α-Fe.

3.6.4 X-Ray Diffraction Analysis

XRD analysis was not performed on the solid filtered through the dead end cell as a larger amount of solid was needed for this analysis than could be recovered from 10mL of original suspension. The solid fraction for the XRD analysis was retrieved from centrifugation of the suspension at 3500rpm for 10 minutes. The supernatant was discarded and the solid sludge was kept separately and accumulated over many centrifuge runs. This sludge was not dried for the XRD analysis, but analyzed while still wet. A representative amount of the sludge was transferred to a quartz sample slide**.** X-ray diffraction was performed with a Scintagdiffractometer with Cu source (λ=1.5418 Å). The X-ray tube was operated at 40 kV and 40 mA using a diffraction beam graphite-monochromator. The data was collected between 2θ values of 5^o to 65^o with a step size of 0.02^o and an average counting time of 1 second per step. Qualitative analysis of the XRD patterns was performed using the Jade software (MDI 2008).

3.6.5 Cr(VI) Reduction by Solid Fraction

The entire NF270 filter with solid retained was immersed in 200mL of 50 mg/L as Cr(VI) solution in a 250mL Erlenmeyer flask and shaken. The pH was measured and 5M $HNO_3$was added dropwise to lower the pH to a value between 2 and 4 if needed. A magnetic stirrer was

added to the flask and sealed with parafilm. The mixture was stirred continuously for 24 hours and then vacuum filtered through a 0.22 μm pore size filter. The resulting solution was diluted by a 1:10 ratio using DI water and the Cr(VI) concentration was measured using colorimetric EPA Method 7196a.

4. Results and Discussion

4.1 Suspension Analysis

4.1.1 Redox Potential and Titration Curves

The redox potentials of the suspensions (Figure 4.1.1) were found to increase with the concentration of iron in solution, ranging from 219 mV for a green tea solution with no iron to 704 mV for a 0.1M Fe^{3+} solution. All solutions were observed to have highly positive redox potential, including the green tea alone. However, as it will be shown in later discussion, the positive Eh does not indicate the complete absence of reductive potential in solution. This redox potential is not representative of an equilibrium state in the solution and the actual redox species present. The remaining dissolved Fe^{3+} in the highly acidic solution dominates the redox potential, potentially masking the reductive species that are also present in solution. The Eh cannot be considered as an indicator for the reductive capacity of GT-nZVI solutions.

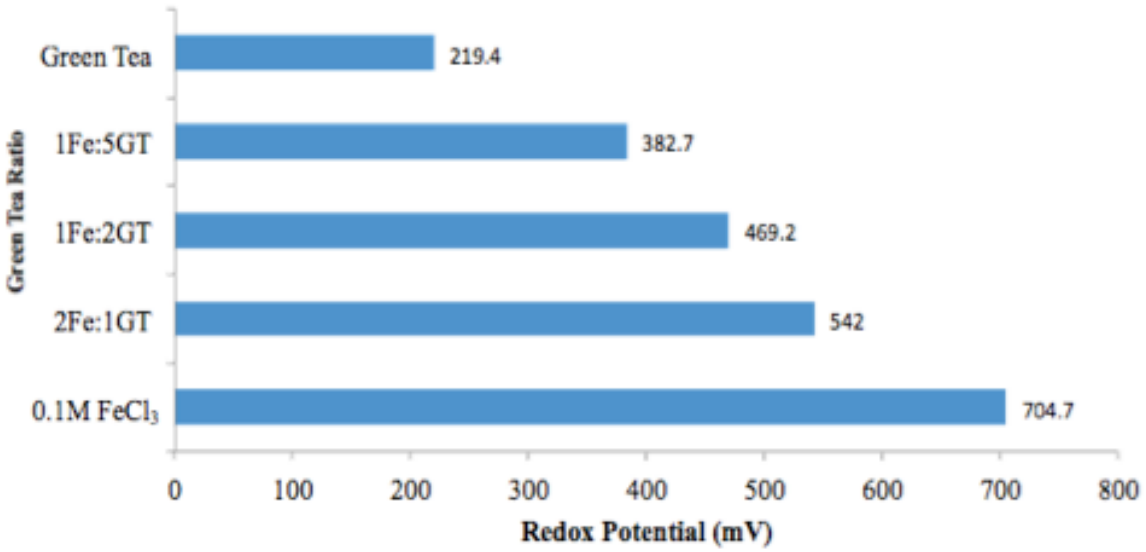

Figure 4.1.1: Redox Potential (in mV) of solutions with varying iron:green tea ratios

All titrations were performed between the natural solution pH (~2) to a pH of over 11 and are shown in Figure 4.1.2. The titration curves showed a very poor buffering capacity of the green tea alone. As the ratio of iron to green tea increased, the buffering capacity increased. Buffering is likely to be caused by the precipitation of Fe^{2+} and Fe^{3+} minerals with increasing pH.Theoretical titration curves of various Fe^{2+} and Fe^{3+} solutions were generated using the Visual MINTEQ software and are also shown in Figure 4.1.2.Modeling was performed in the absence of CO_2 and organic matter, both of which are likely to play a role in the speciation of Fe. Theoretical titration curves in the presence of carbonate were attempted, but produced very poor agreement at higher pH values and are thus not shown. A 66mM $FeCl_3$ solution was predictedto have two plateaus, which correspond to the precipitation of different minerals. At pH 2, an iron chloride hydroxide ($Fe(OH)_{2.7}Cl_{0.3}$) is predicted to precipitate, which is replaced by hematite (α-Fe_2O_3) at pH 7. For a pure Fe^{2+} solution a single precipitate is predicted ($Fe(OH)_2$) at all pH values except the initial equilibration point of pH 5.5, at which Fe^{2+} is still entirely dissolved. In the presence of both Fe^{3+} and Fe^{2+} magnetite (Fe_3O_4), a mixed-valence mineral, is predicted to

start precipitating at pH 4 and remains stable for the entire titration curve, while $Fe(OH)_2$ also precipitates at pH higher than 7.5.

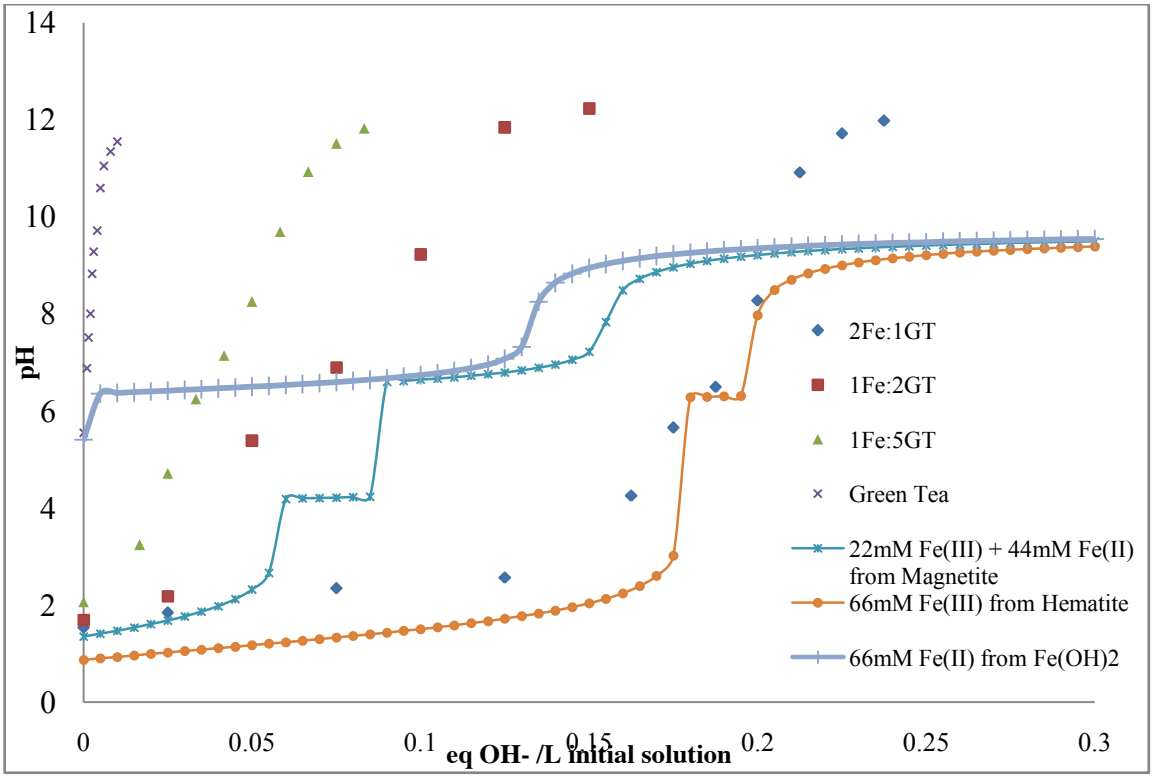

Figure 4.1.2: Titration curves of solutions with various tea-Fe ratios and theoretical titration curves of Fe^{3+} and Fe^{2+} solutions

The comparison of the experimental with the theoretical curves is limited by the small number of data points. There are several additional limitations: organic matter was not include in the model, carbonate is likely to play a role in the neutral pH range, and the suspensions are unlikely to have reached equilibrium, especially at the lower pH values where Fe precipitation is kinetically slow. A suspension that had been completely converted to Fe^{2+} would have a higher initial pH, but none of the suspensions have an initial pH above 2, so there must be Fe^{3+} present in all of these suspensions. The 2Fe:1GT suspension most closely resembles the full 66mM Fe^{3+} curve out of the three samples; the higher initial pH may be from the contribution of the green tea solution or form the presence of some Fe^{2+}. The 1Fe:2GT and 1Fe:5GT curves are

intermediate curves between the pure Fe^{3+} and the pure green tea, with likely contribution from all three components (Fe^{2+}, Fe^{3+} and green tea).

4.1.2 XANES Analyses

Interpretation of XANES spectra is performed using comparison with standards of known valence state and structure. This may be done qualitatively, by comparing the absorption energies of single valence compounds with the observed spectra, or quantitatively, by performing Linear Combination Fitting (LCF) of the observed spectra using spectra of pure compounds. In this case, LCF could not be performed, because the available Fe XANES spectra of oxides, hydroxides and dissolved species were not present in the suspension, as indicated by the Mössbauer spectra shown in a subsequent section. Thus, only a qualitative analysis of the obtained spectra was performed. These are shown in Figure 4.1.3. Several reference spectra are shown in Figure 4.1.4 and the characteristic energies of eachas derived from the first derivative spectra are summarized in Table 4.1.1. It should be noted, however, that the characteristic energy of 7112 eV for Fe^0 does not imply the complete absence of such a feature in higher valence compounds. In fact, Figure 5.2.3b shows that all compounds present small peaks at that energy, albeit with lower intensity.

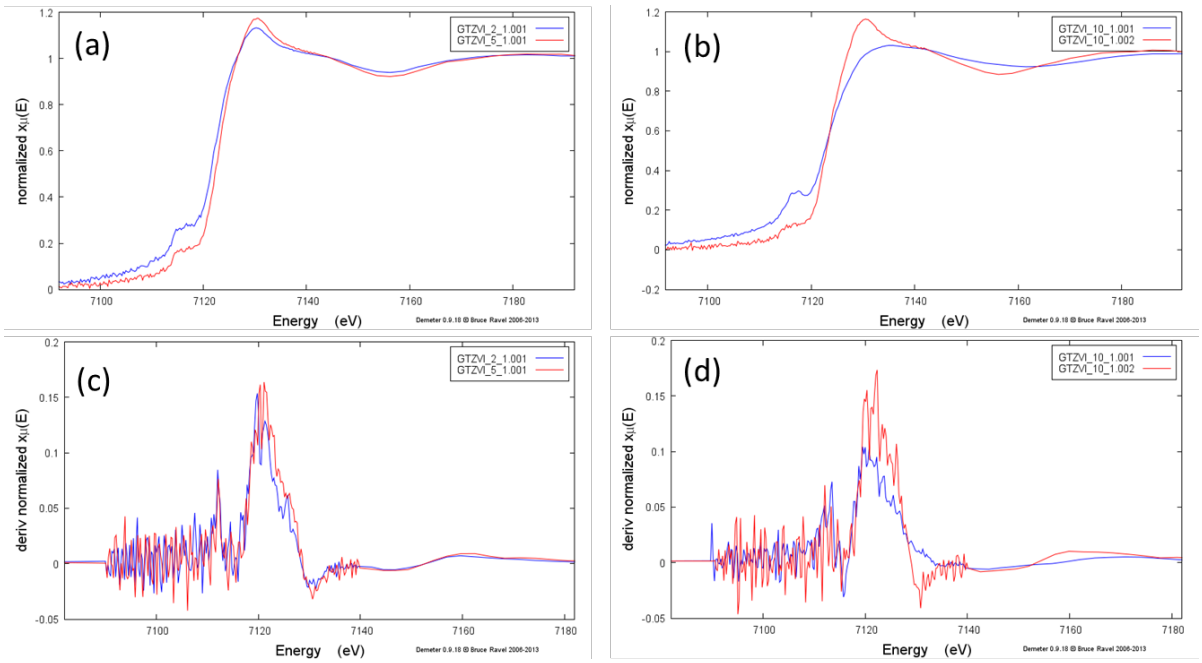

Figure 4.1.3: XANES spectra of samples 1Fe:2GT and 1Fe:5GT (a) and their first derivative (c) and of consecutive scans of sample GT10:Fe1 (b) and their first derivative (d)

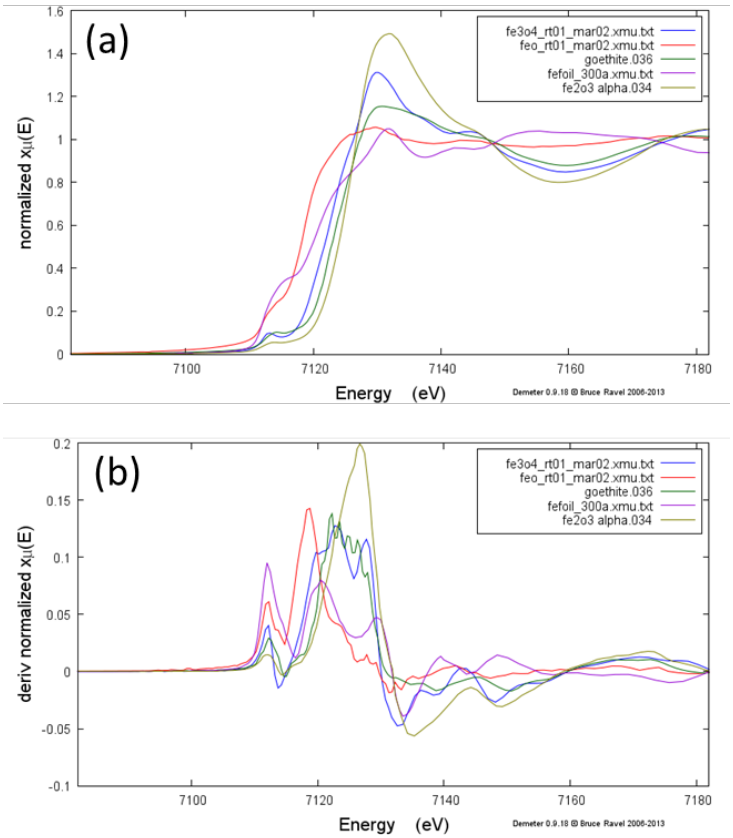

Figure 4.3.2: XANES reference Spectra of Iron Species from GCAS-Newville and IIT Database (a) and their first derivative (b)

Table 4.1.1: Characteristic energies of Fe valence states derived from the first derivative spectrum of various minerals

Mineral	E_{Fe0}(eV)	E_{Fe2+} (eV)	E_{Fe3+} (eV)
Iron foil	7112		
$FeSO_4$ (solution)		7118.8	
FeO		7118.6	
Fe_3O_4		7119.5	7123.0
Fe_2O_3			7121.9, 7125.2
Goethite (α-FeOOH)			7122.0

The first derivative spectra of both samples 1Fe:2GT and 1Fe:5GT present two peaks, the highest at 7119.5 eV and the second one at 7112 eV. The 7119.5 eV peak is consistent with the presence of a mixed valence compound (Fe^{2+} - Fe^{3+}). As it will be shown later, Mössbauer spectroscopy indicated that no oxides were present in the two samples, so that the peak comparison is only performed on the basis of valence state and not actual mineral presence. The relative height of the 7112 eV compared to the 7119.5 eV peak is higher compared to the relative heights of the respective magnetite peaks (Figure 4.3.2). This may be an indication that some Fe^0 is present in the sample as well, however the lack of proper organometallic Fe XANES standards renders a conclusive statement difficult. In any case, Fe^0 is certainly not a predominant species in the two analyzed suspensions.

The first derivative of the first scan of sample 1Fe:10GT showed the highest peak at 7119.5 eV, while the second scan was shifted to 7122.5 eV. This is indicative of beam damage, i.e. progressive oxidation of Fe due to subsequent scans of the same sample. For this reason, all other samples were analyzed with only a single scan. A second smaller peak was also present at 7112 eV and its relative intensity to the 7119.5 eV peak in the first scan was considerably higher compared to the samples 1Fe:2GT and 1Fe:5GT. This might be an indication that Fe was in a more reduced state in this sample and that Fe^0 might be present. Still, a mixed Fe(II)-Fe(III)

species was again predominant in the 1Fe:10GT sample as well.

4.2 Liquid Fraction Analysis

4.2.1 Iron Oxidation in Liquid Fraction

The average results of the Ferrozine assay for $Fe^{2+}$and Flame Atomic Absorption Spectroscopy (FlAAS) for total Fe are shown in Figure 4.2.1along with standard deviations. The concentration of Fe^{3+} was obtained by subtracting the concentration of Fe^{2+} from the total iron. The standard deviations were quite high compared to the average values for all solutions and for both Fe^{2+} and total Fe, indicating a wide variability in the liquid properties. There are two potential sources of spread: variability in the degree of Fe reduction and precipitation, and variability in the filtering efficiency.

The total iron in the liquid effluent increased as the iron ratio increased in the original suspension. The percentage of iron recovered in the outflow from the initial suspension was, however, on average approximately the same for the three mixtures (20% for 1Fe:5GT and 2Fe:1GT and 26% for 1Fe:2GT). The distribution of iron species was, however, different. 1Fe:5GT and 1Fe:2GT liquid samples had more Fe^{2+} than Fe^{3+} on average. The 2Fe:1GT liquid sample had almost equal Fe^{2+} and Fe^{3+} with slightly more Fe^{3+}. These observations agree with the titration curves presented in Figure 4.1.2, which showed a dominance of Fe^{3+} in the overall suspension of 2Fe:GT1.

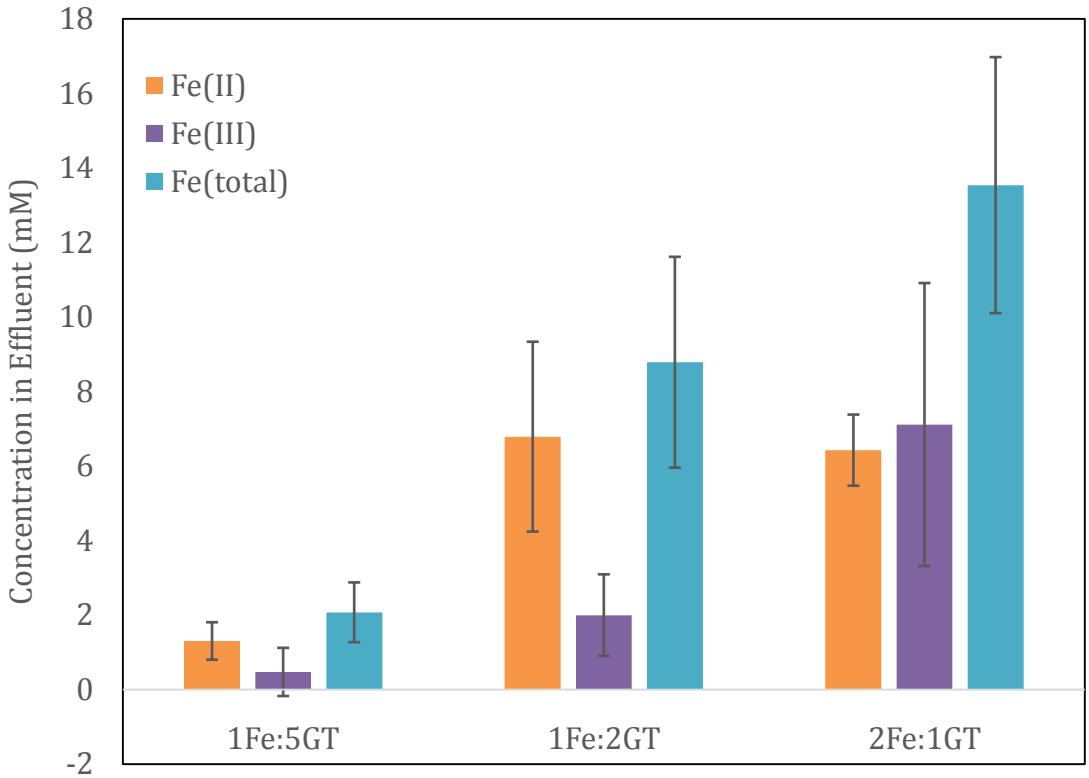

Figure 4.2.1: Concentration of Iron Species in Liquid Effluent

As discussed in the literature review, green tea has reductive capabilities due to polyphenol interactions. Based on the Folin-Ciocalteu assay, a solution of the Chunmei Special Grade green tea used in this research has an average polyphenol content ranging from 2-2.8 mg/L gallic acid equivalents (GAE), varying with the tea leaf concentration and time brewed. The green tea solution used in experiments was brewed at a concentration of 20 g/L for 30 minutes at 80 ^{o}C and had an average of 2.61 g GAE/L, which is equal to 15.33 mmol [PH]/L in the green tea solution using the gallic acid molecular weight of 170 g/L. As detailed in the literature review, the Fe reduction potential of green tea depends on the relative concentration of the different polyphenols and on the molar ratio of the polyphenols to the total iron concentration. Low MW compounds such as catechol produce 1 or 2 mols of Fe per mol of compound, while high MW weight compounds produce 1 to 4 mol of Fe per mol depending on

the Fe:compound ratio (Ryan and Hynes, 2001). Based on the analysis shown in Table 2.2.1, we will assume that 33% of the polyphenols behave like EGCG and the remaining like catechin. In the 1Fe:5GT suspension, the Fe:PH ratio is quite low, so that the maximum production of Fe^{2+} is 1 mol per mol of PH for both high and low MW compounds. For the 1Fe:2GT suspension, 1 mol of low MW compounds could produce up to 2 mols of Fe^{2+}, while 1 mol of high MW compounds could produce up to 3 mols of Fe^{2+}. In the 2Fe:1GT suspension, the values are 2 for low MW and 4 for high MW compounds, respectively. The resulting theoretical reduction of the total initial iron concentration based on the above analysis is shown in Table 4.2.1.

Table 4.2.1: Theoretical Reduction of Fe by Polyphenols in 20 g/L Green Tea Solution

Fe:GT ratio	[PH] mmol/L	[Fe] mmol/L	Fe:PH Molar Ratio	Theoretical mmol/L of total Fe^{2+} produced	Theoretical mmol/L of total Fe^{2+} in liquid	Average Actual mmol/L of Fe^{2+} in Liquid Fraction	Theoretical % of Fe^{2+} produced	Average Actual % Fe in Liquid Fraction
1Fe:5GT	12.77	16.67	1.31	12.77	2.55	2.52	77%	81%± 29%
1Fe:2GT	10.22	33.33	3.26	20.44	6.19	6.79	71%	76%± 11%
2Fe:1GT	5.12	66.66	13.05	15.36	2.72	6.42	20%	51%± 18%

In addition, the liquid analysis results indicated that 20-26% of the total initial iron went through the filter. Multiplying these values with the total theoretical production of Fe^{2+}, we calculated the theoretical concentration of Fe^{2+} in the liquid effluent based on the polyphenol content. The fractions of the Fe^{2+} of the total initial and observed Fe in the suspension and effluent are also shown in Table 4.2.1.

The results of this analysis indicate that the concentration of the Fe^{2+} in the effluent is in agreement with the theoretical approach for the 1Fe:5GT solution and in quite close agreement

for the 1Fe:2GT solution. However, in the 2Fe:1GT solution, the observed Fe^{2+} in the effluent is double the theoretical value. This indicates that the efficiency of the reduction reaction increases with the Fe content, even though the total polyphenol content available is drastically reduced. This is likely because of the ratio of iron:green tea being in a range where the polyphenols act in a 1:4 reduction ratio as discussed in the literature review. Still, the polyphenol content is too low to reduce all the available iron, so that a large excess of Fe^{3+} remains in solution. It appears that the 1Fe:2GT mixture constitutes an optimal compromise between optimizing the efficiency of the polyphenols and having enough concentration to minimize the excess Fe^{3+} remaining in solution. The presence of large quantities of Fe^{3+} is undesirable for any remediation application, because its superfluous precipitation causes soil and water acidification and clogging of porous media.

4.3 Solid Fraction Analysis

4.3.1 XANES Analysis Results for Solid Fraction

The XANES analysis of the solid fraction was performed similar to the suspension, by comparing the peak energies of the first derivative spectra with the energies of the various oxidation states. Again, assignment of particular minerals was not done given that Mössbauer analysis (see next section) precluded the presence of oxides except in the 2Fe:1GT sample.

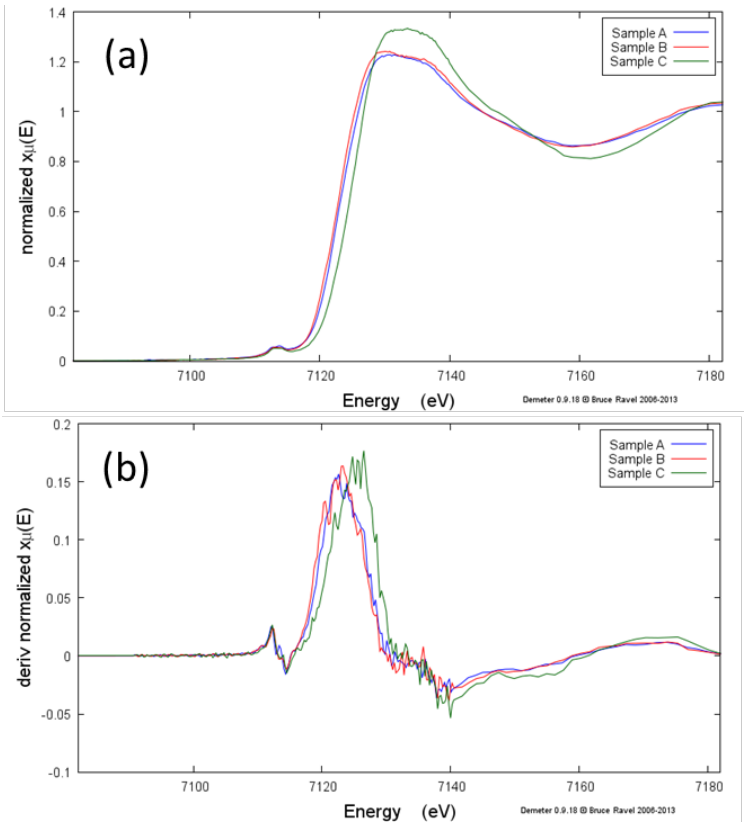

Figure 4.3.1: Fe K edge XANES spectra (a) and first derivatives (b) of solid fraction of samples 2Fe:1GT (A), 1Fe:2GT (B) and 1Fe:5GT (C)

The spectra of samples 2Fe:1GT and 1Fe:2GT were identical, with the highest peak at 7122.5 eV and a considerable smaller peak at 7112 eV. The highest peak of sample 1Fe:5GT was at 7125.5 eV, with the second peak at 7112 eV. The shift towards higher energies is indicative of a higher degree of oxidation.

The comparison with the energies at Table 4.2.1 indicates that iron is mostly Fe(III) in all samples. However, comparison of the original spectra shows that the spectrum is shifted to the left compared to the spectra of pure Fe(III) compounds, so that a mixed-valence Fe(II)-Fe(III) species is more likely. The comparison with the spectra of the full suspensions in Figure 4.2.1 shows that the solid fraction spectra are oxidized compared to the full suspension. This indicates some loss of the Fe(II) and of any Fe^0 from the original suspension due to the filtration and

drying of the sample. This conclusion agrees with the observations of the Cr(VI) reduction experiments described later on.

It should be noted that XANES is the only spectroscopic analysis that could be performed in the original suspension. Mössbauer, XPS and XRD all require a solid sample. So while these methods cannot provide an accurate indication of the relative percentages of the various valence states in the solid sample, they can provide information with regard to the actual structure of Fe, which XANES cannot do because of the lack of appropriate standards. Thus, all used methods operate in a complementary fashion to draw conclusions on the speciation and reactivity of Fe in the GT-Fe suspension. All other analyses of the solid will be presented with this caveat.

4.3.2 Mössbauer Analysis Results for Solid Fraction

Two sets of Mössbauer analyses were performed. The first set was performed at room temperature on solid obtained from centrifugation of the suspensions and nitrogen drying. The second set was performed on solids obtained from filtration at four different temperatures (295 K, 140 K, 80 K and 4 K). The different temperatures are employed in order to investigate changes in the magnetic ordering, which may reveal additional properties of the Fe species (Dyar et al., 2006). Figure 4.3.2 shows the Mössbauer spectra for the first round of analyses and Table 4.3.1 summarizes the Mössbauer parameters fitted from the spectra.

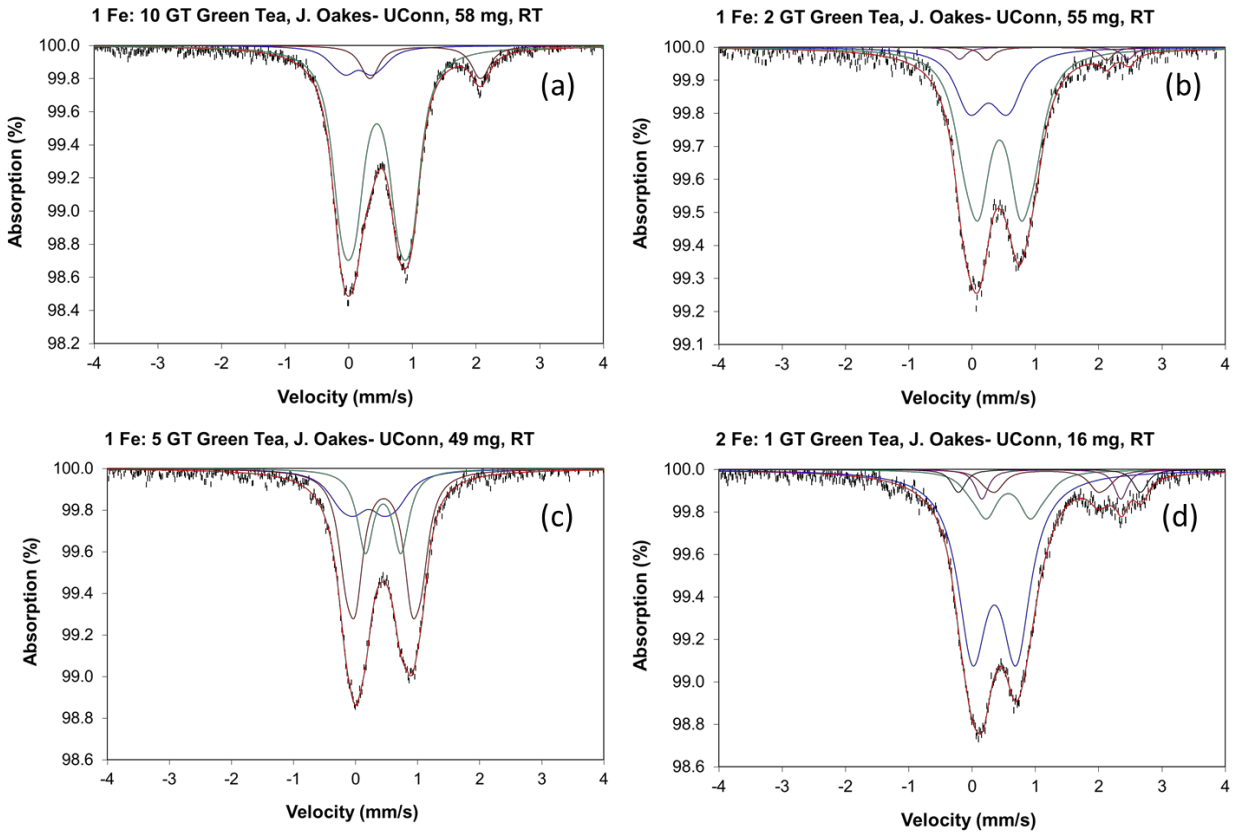

Figure 4.3.2: Room temperature Mössbauer spectra of GT-Fe samples after centrifugation and N_2-drying

Table 4.3.1: Mössbauer parameters fitted from the room temperature spectra of centrifuged GT-Fe samples

Sample		**1 Fe: 10 GT**	**1 Fe: 2 GT**	**1 Fe: 5 GT**	**2 Fe: 1 GT**
Velocity scale (mm/s)		+/- 4	+/- 4	+/- 4	+/- 4
Temp (K)		295	295	295	295
Ferric 1	**IS***	0.15	0.26	0.21	
	QS*	0.38	0.71	0.42	
	Width	0.40*	0.49	0.51	
	Area	10	26	24	
Ferric 2	**IS**	0.44	0.43	0.44	0.35
	QS	0.61	0.63	0.56	0.70
	Width	0.33	0.42	0.30*	0.55
	Area	81	69	24	69
Ferric 3	**IS**			0.45	0.57
	QS			0.90	0.70
	Width			0.300*	0.40*
	Area			53	15
Ferrous 1	**IS**	1.20	1.18		1.18
	QS	1.73	1.90		1.61
	Width	0.30*			0.33

	Area	9	3		6
Ferrous 2	**IS**		1.15		1.27
	QS		2.66		2.18
	Width		0.23**		0.23**
	Area		2		5
Ferrous 3	**IS**				1.24
	QS				2.88
	Width				0.23*
	Area				4
	$\mathbf{X^2}$	596.79	497.96	596.13	533.07
	$\mathbf{\lvert X^2 \rvert}$	1.16	0.97	1.16	1.04
	$\%Fe^{2+}$	**9**	**5**	**0**	**16**

*IS: Isomer Shift QS: Quadruple Splitting **parameter fixed

The spectra indicated that there was ferrous iron present in all samples except the 1Fe:5GT and that the highest concentration was observed in the 2Fe:1GT sample. The second important observation was that no iron oxide or hydroxide was observed in any of the spectra. These compounds typically have six characteristic peaks called "sextets" (Dyar et al. 2006), which were absent from all spectra. This finding was further investigated through the low temperature analyses, which are more suitable for oxide identification. The low-temperature spectra are shown in Figure 4.3.3 and the corresponding parameters in Table 4.3.2.

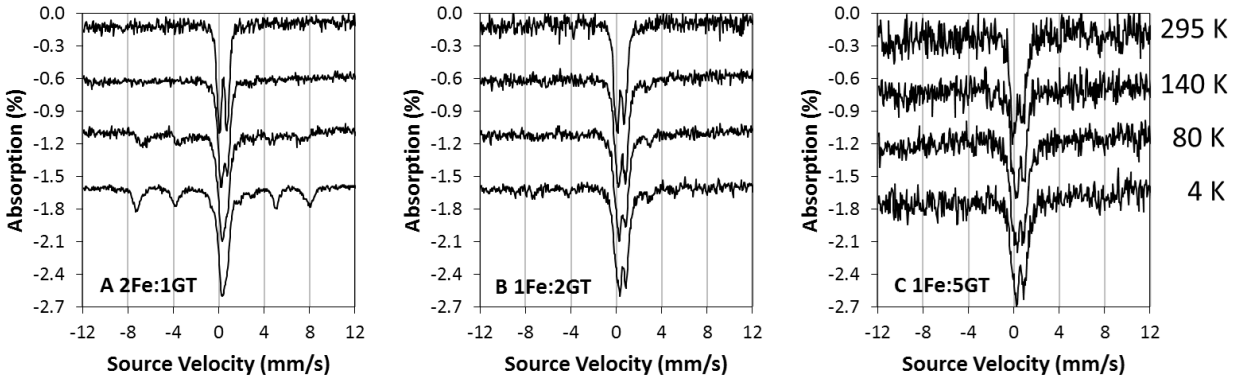

Figure 4.3.3: Variable temperature Mössbauer spectra of samples 2Fe:1GT (A), 1Fe:2GT (B) and 1Fe:5GT (C)

Table 4.3.2: Mössbauer parameters fitted from variable temperature spectra of nanofiltered GT-Fe samples

Sample		A, 2Fe:1GT	A, 2Fe:1GT	B, 1Fe:2GT	C, 1Fe:5GT
Velocity Scale (mm/s)		+/- 12	+/- 12	+/- 12	+/- 12
Spectrum Temp (K)		295	4	295	295
Ferric	**IS**	0.38	0.43	0.34	0.25
	QS	0.49	0.46	0.35	0.35
	Width	0.29	0.62	0.32	0.50
	Area	42	58	39	30
Ferric	**IS**	0.38		0.37	0.36
	QS	0.90		0.94	1.00
	Width	0.35		0.40	0.47
	Area	58		61	70
Ferrous	**IS**		1.62		
	QS		2.62		
	Width		0.31		
	Area		4		
Akaganéite	**IS**		0.51		
	QS		-0.53		
	Field		453.5		
	Width		0.62		
	Area		12		
Akaganéite	**IS**		0.48		
	QS		-0.19		
	Field		486.6		
	Width		0.47		
	Area		26		
	c^2	570.7	675.5	494.1	468.9
	c^2_{norm}	1.1	1.3	1.0	0.9
	% Fe^{2+}	**0**	**4**	**0**	**0**

*parameter fixed

These analyses confirmed that no (hydr)oxides were present in the 1Fe:2GT and 1Fe:5GT samples, while the 2Fe:1GT sample exhibited a sextet at the lower temperatures. The peaks are thought to be characteristic of akaganéite (β-FeOOH) (Darby Dyar, personal communication). The presence of ferrous iron was less pronounced in the second set of spectra for two reasons: a) the spectra were obtained at a lower resolution of 12 mm/s (vs. 4 mm/s for the first set, increasing spectral noise and rendering fitting of the smaller ferrous peaks difficult); b) filtration

causes iron oxidation, as described in the XANES analysis. However, this second set of analysis is confirmation that the formation of oxides is not favored in the Fe-GT suspensions, with the exception of the high iron 2Fe:1GT sample.

These findings are consistent with previous Mössbauer investigations of iron interactions with catechol, pyrogallol, gallic acid and tannins, a sub-group of polyphenols (Gust and Suwalski 1983, Jaen et al. 2009, 2011). Gust and Suwalski reported the formation of two Fe(III)-polyphenol complexes that had similar Mössbauer parameters regardless of the type of polyphenol reacted and described these as CI and CII complexes without further describing the nature of the complexes. The same authors reported reduction of Fe(III) to Fe(II) and precipitation of ferrous sulfate, since the original reagent was ferric sulfate. The Mössbauer parameters of the two complexes are shown in Table 4.3.3.

Table 4.3.3: Mössbauer parameters of Fe-polyphenol complexes reported by Gust and Suwalski (1983)

Temperature (K)	Compound	QS (mm/s)	IS (mm/s)
78	CI	0.78 ± 0.07	0.55 ± 0.03
	CII	1.21 ± 0.08	0.56 ± 0.04
300	CI	0.80 ± 0.06	0.43 ± 0.02
	CII	1.19 ± 0.08	0.44 ± 0.02

Comparing the parameters reported by Gust and Suwalski (1983) for 300 K with the parameters in Table 4.3.1 it appears that the species described as “ferric 2” likely corresponds to the CI complex and was present in all four Fe:GT ratios. In three of those (2Fe:1GT, 1Fe:2GT and 1Fe:10GT), it was the largest contribution to the peaks, as evidenced by the corresponding area. There were no parameters that appeared to match the CII complex in the any of the samples.

Jaen et al. (1999) studied the interaction of a variety of plant extracts with ferrous and ferric sulfate solution and confirmed the presence of compounds with similar

Mössbauerparameters. The interaction of some extracts yielded only the CI type (Tuna, Pitahaya, CedroEspino and Acacia), while other yielded both types. The compositional differences between the various extracts were not reported. The authors also reported that the plant extracts inhibited the formation of oxides and hydroxides and Jaen et al. (2003) later observed that the inhibition occurred when the polyphenol concentration exceeded 1%. The spectra reported by Jaen et al. (2003) and (2009) were very similar to the ones presented in this study. Thus, the main findings from the Mössbauer analysis are:

- The interaction of polyphenols with iron produces organic complexes, while the formation of oxides and hydroxides is inhibited, except at high iron concentrations.
- There was no evidence of formation of zero valent iron in any sample investigated.
- Both ferrous and ferric iron were identified, with the proportion of ferrous quantified between 5 and 16%. The higher percentage corresponded to the 2Fe:GT1 mixture. It is likely that additional ferrous iron is present in the original suspension but is oxidized due to the sample preparation process.

4.3.3 XPS Analysis Results on Solid Fraction

XPS analysis was performed on the solid fraction of the 2Fe:1GT, 1Fe:2GT, and 1Fe:5GT multiple times. There were two major challenges in performing the spectral analysis: calibration of the spectrum based on the graphite peak was difficult because of the overlap with the carbon energies of the various types of carbon energies in the polyphenol groups; and, iron peaks were very small because of the low amount retained in the solid compared to the amount of organic matter. Thus, interpretation of the XPS spectra could only be done in the context of the XANES and Mössbauer analyses, i.e. taking into account information obtained from these methods.

Figure 4.3.9 is one of the full survey (all element) scans of the 2Fe:1GT sample and is characteristic of what the full survey looked like for all of the samples scanned, with slight differences in the prominence of peaks shown.The blue shaded areas represent the regions over which a specified element could have a potential peak and the region that high resolution analysis is performed following the full survey analysis. All scans showed an obvious and pronounced carbon peak. The scans with a higher green tea ratio had a larger oxygen peak. Some scans showed a chloride peak as well. Iron was found in all scans under high resolution. However, the iron was frequently undetectable as a peak on the full survey, as it was not the most abundant element in the sample. This particular scan actually has a more prominent iron peak than in most of the scans.

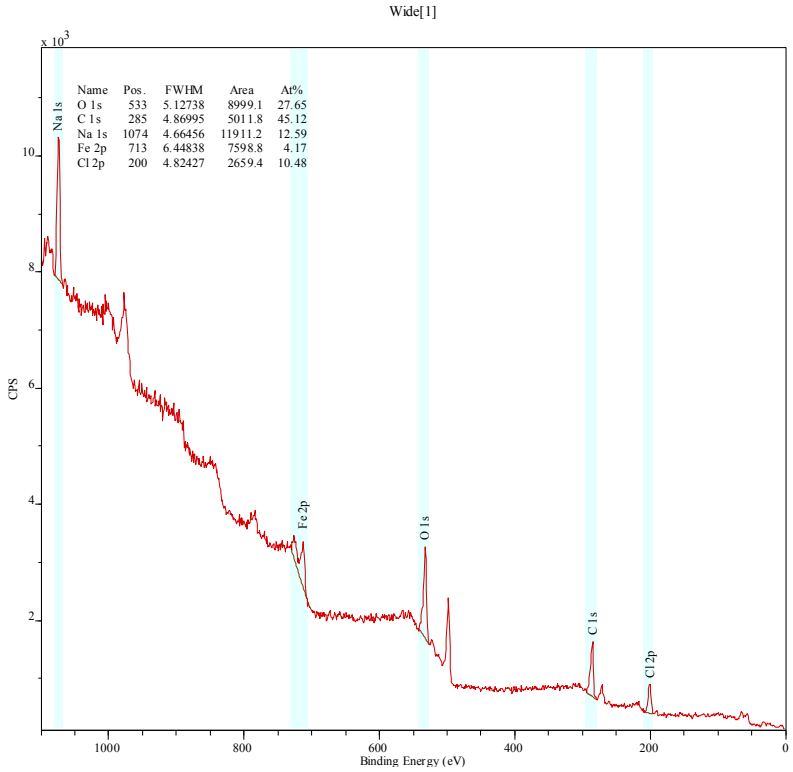

Figure 4.3.9: Characteristic Full Survey of All Sample Scans

Two high-resolution scans were obtained for each sample, one for the carbon peak and

one for the iron peak. The carbon analysis is used to calibrate the energy of the scan, assuming that the most prominent peak corresponds to the graphite C_{1s} energy of 284.6 eV. Graphite is the carbon substrate used to mount the sample and is thus present in all scans irrespective of the sample. The difficulty associated with this assumption is that the observed carbon peaks were the result of several overlapping carbon energies.The observed wide peak may be modeled using different combinations of smaller peaks with a full-width at half maximum (FWHM) around 2 eV, and then the highest of the fitted peaks is assumed to be graphite, given that the mounting tape should contribute the majority of the observed counts. However, this is an assumption that cannot be independently verified.

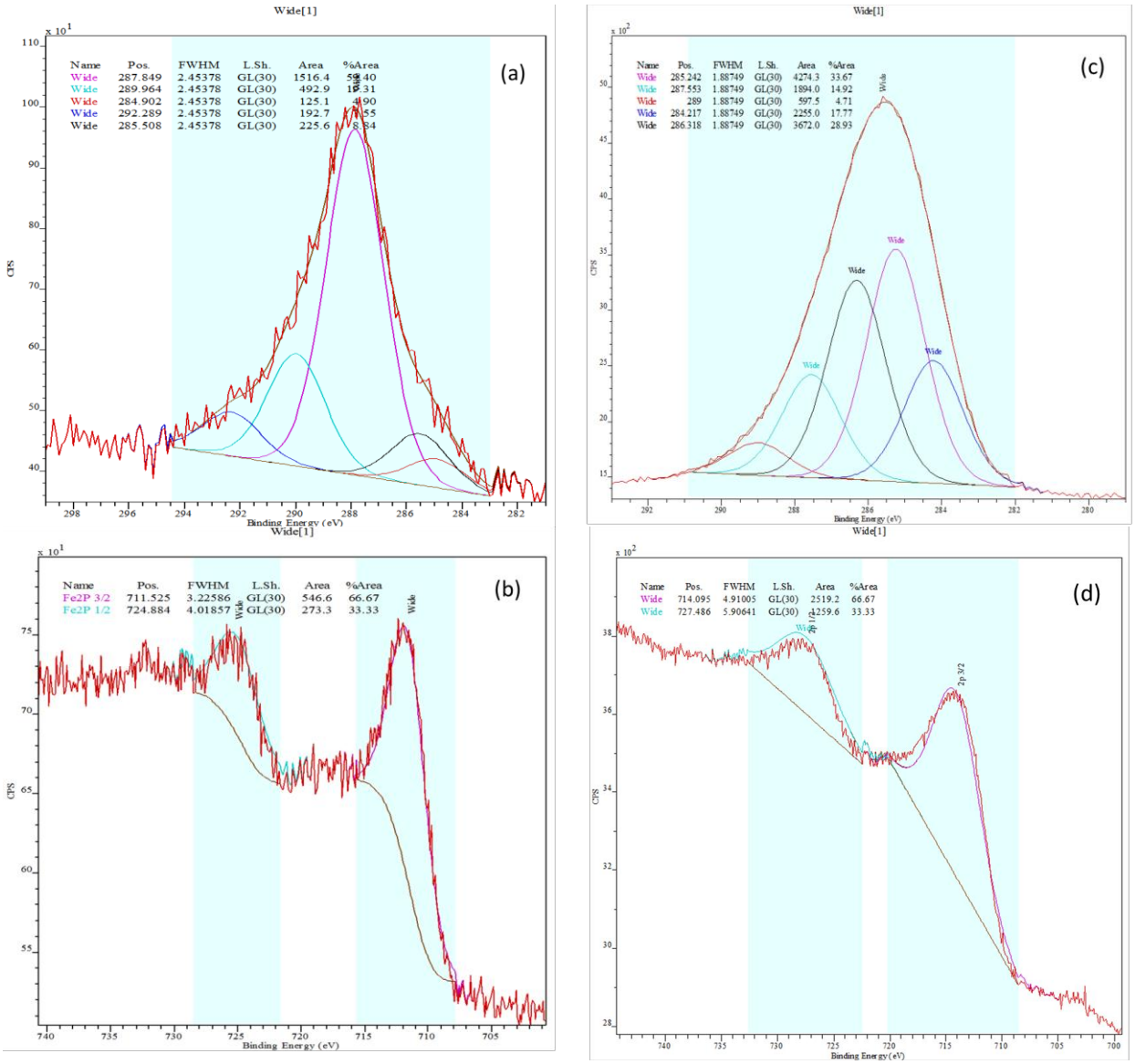

Figure 4.3.10: XPS High Resolution Scans of Carbon (a,c) and Iron (b,d) for 2Fe:1GT Solid Sample

Figure 4.3.11 shows the carbon and iron scans of two sub-samples of 2Fe:1GT. The carbon peak of the first scan (Fig. 4.3.11a) had a centroid at 288.0 eV and a FWHM of 3.4 eV. This peak was modeled as five overlapping peaks and the largest peak was centered at 287.85 eV. This yielded a shift of 3.25 eVtowards lower energies that was applied in the corresponding Fe peak (Fig. 4.3.11b). It should be noted that this shift is quite large, which renders the reliability of the analysis low. Using this shift, the two Fe peaks were centered at 711.5 eV and 724.9 eV.

The two peaks correspond to the 2p3/2 and 2p1/2 energy states of a single species, respectively. The FWHM of both peaks were also high, at 3.2 eV and 4 eV. This likely indicates that there are more than one Fe species in the sample and that the peaks should be modeled using two peaks. Doing so yielded energies of 711.1 eV and 713.0 eV for the 2p3/2 peak, and 724.6 and 726.9 eV for the 2p1/2 peak. However, the FWHM remained quite high, thus the fitting is not considered a substantial improvement. However, some conclusions may still be derived by comparing the peak positions with some key iron species shown in Table 4.3.3.

Table 4.3.3: Binding Energies for Iron Species for Spectral Lines 2p 3/2 and 2p 1/2

2p 3/2			**2p 1/2**	
Fe	707.243		Fe2O3	724
FeO	709.829		FeOOH	724.3
Fe2O3	710.961		Fe3O4	723.5
Fe3O4	709.88			
FeOOH	711.37			
FeCl3	711.55			

The binding energy for ZVI is at 707.2 eV. Even with a large shift of 3.25 eV toward lower energies, the Fe peak was centered at 711 eV and no intensity was observed at 707 eV. This means that with all aforementioned uncertainties, the presence of Fe^0 in the analyzed sample can be excluded with certainty. The analysis also indicates that ferrous iron is likely not present in the sample, since its binding energy is around 709.9 eV. The 711.5 eV may belong to FeOOH or $FeCl_3$, which is consistent with the Mössbauer analysis that showed akaganéitein this sample. A search in the XPS database of the National Institute for Standards and Technology (NIST) for

this peak position also yields for several organometallic Fe compounds, for example tris(1-phenyl-1,3-butanedionato-O,O1)iron [Fe((C_6H_5)C(O)CH_2C(O)CH2)$_3$] (Blomquist et al., 1983) at 711.4 eV. At higher energies Sivastava et al. (1985) reported a binding energy of 712.6 eV for tris(2,4-pentanedionato-O,O')iron[Fe(CH3C(O)CHC(O)CH3)3]. Thus, it is considered likely that the polyphenol-Fe complexes identified by Mössbauer spectroscopy present their binding energies in this region.

A second analysis of the 2Fe:1GT sample (Figure 4.3.10b and d) yielded a carbon peak centered at 286.5 eV, which was also modeled with five peaks. The two largest peaks were located at 285.24 eV and 286.32 eV, so that the most likely shifts were 0.64 eV and 1.72 eV towards lower energies, respectively. The 0.64 eV shift had an iron peak was centered at 714.09 eV. The 1.72 eVshift had the iron peak located at 713.0 eV. In either case, we can safely conclude that no ZVI or ferrous iron was present in the sample and that the Fe compound was again most likely organometallic.

The XPS analysis of the 1Fe:2GT (Figure 4.3.11) and 1Fe:5GT (Figure 4.3.12) samples was even more problematic, because the lower amount of iron and the higher contribution of organic matter rendered calibration even more difficult. However, similar observations could be drawn in those cases as well using the same line of arguments as for the 2Fe:1GT sample, i.e.:

- All carbon spectra had energies centered at energies higher than the graphite peak (292.0 eV and 287.8 eV for 1Fe:2GT, and 288.2 eV and 292.5 eV for 1Fe:5GT). This means that any applied shift will be towards lower energies, so that Fe^0 or Fe^{+2} will not be missed because of the shift. If anything, reduced species might be falsely identified (which is not the case, as will be discussed).

- The Fe peaks are centered around 711 eV for 1Fe:2GT (Fig.4.3.11b,d) and around 710 eV for 1Fe:5GT (Fig. 4.3.12b,d). For all cases, the presence of ZVI can be safely excluded, while Fe^{2+} is likely present, but not the predominant species. Again, Fe-polyphenol complexes or organometallic compounds are the most likely species to account for the observed positions.

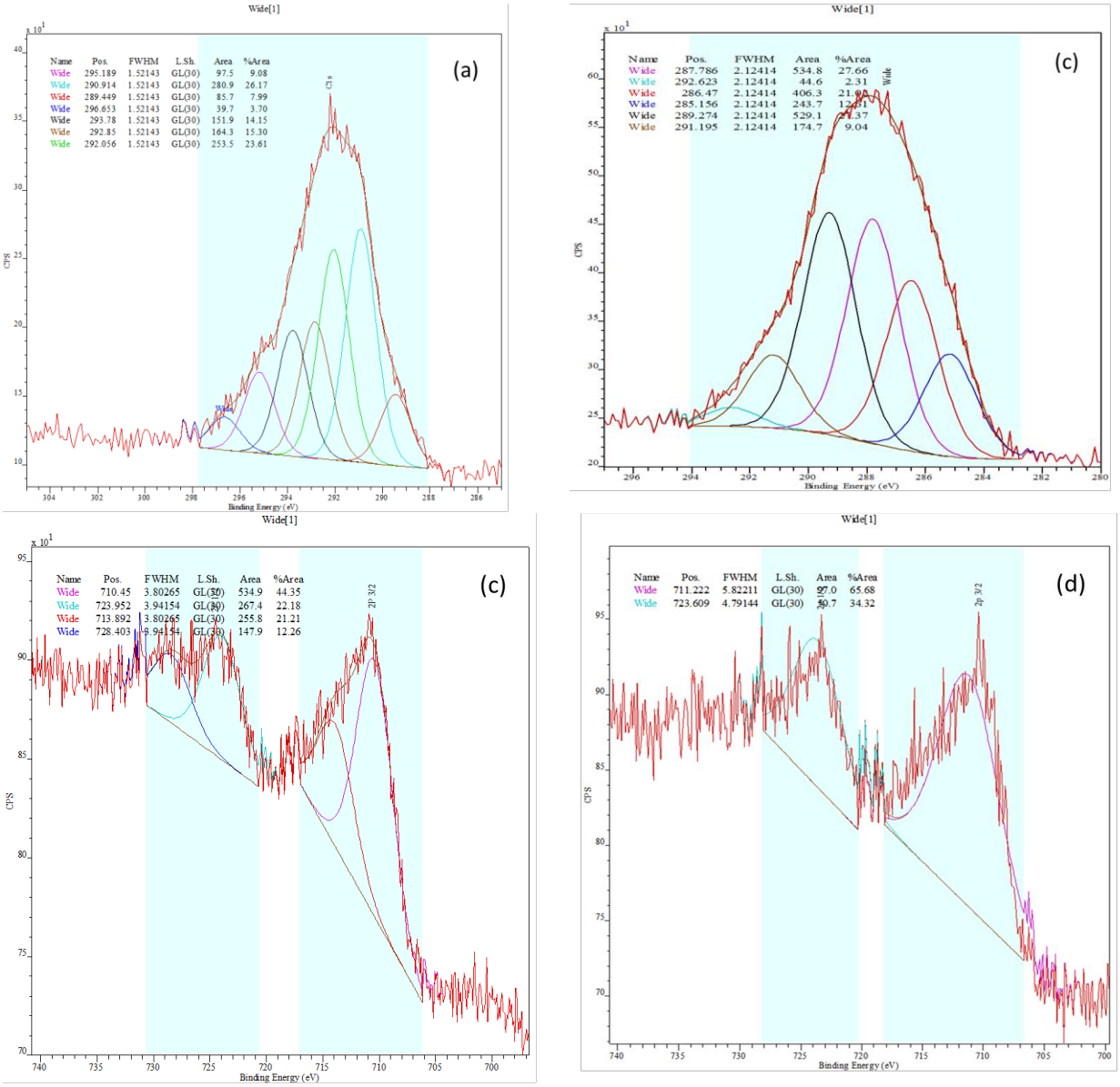

Figure 4.3.11: XPS High Resolution Scan of Carbon (a,c) and Iron (b,d) for 1Fe:2GT Sample

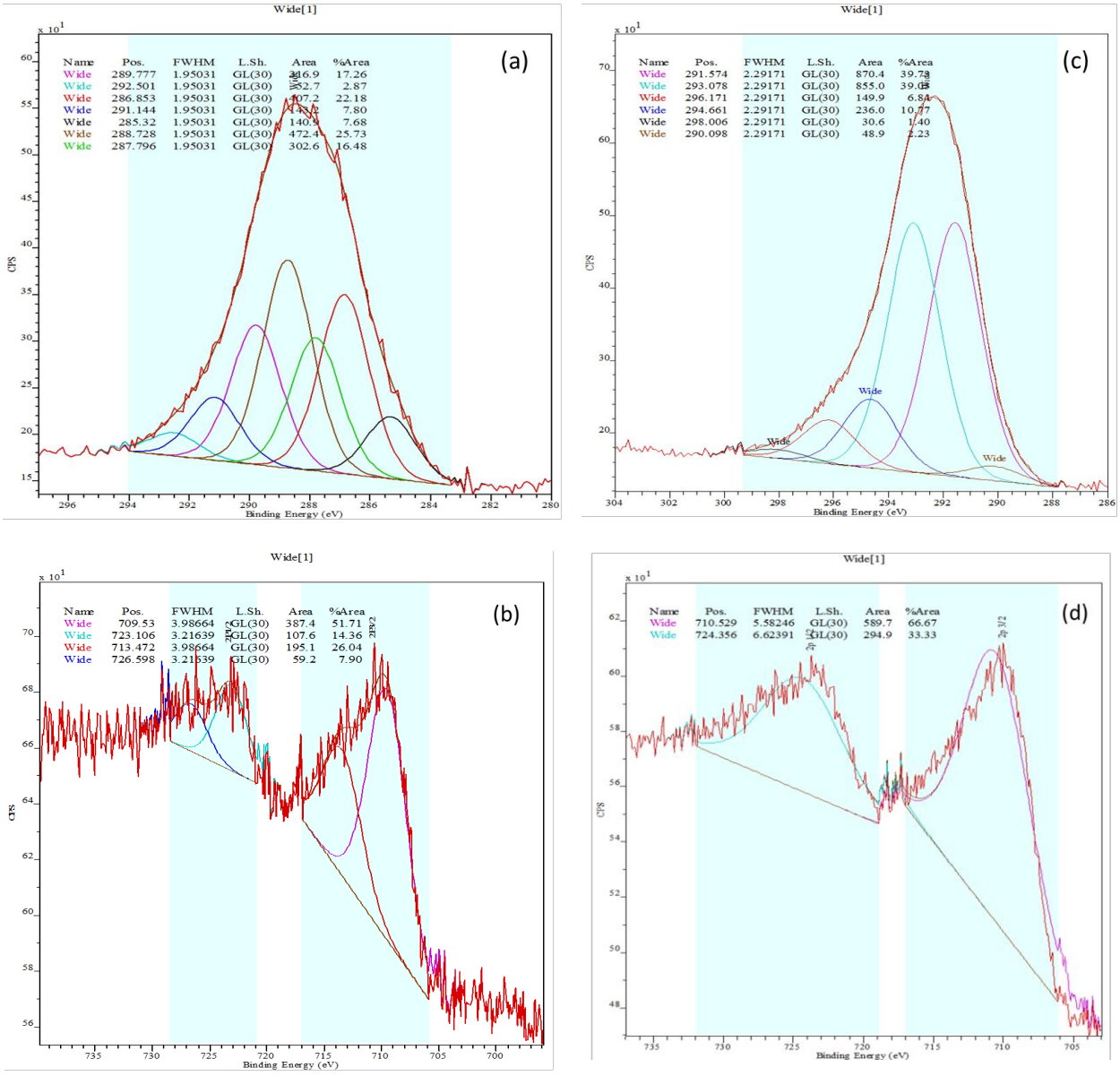

Figure 4.3.12: XPS High Resolution Scan of Carbon (a,c) and Iron (b,d) for 1Fe:5GT Sample

4.3.4 XRD Analysis Results on Solid Fraction

X-ray diffraction analysis did not show any metallic iron or any crystalline structure present in the sample sludge. The resulting scans show only an amorphous scan with a wide organic peak surrounding quartz, which is the material of the sample cell. Figure 4.3.13 shows the 2Fe:1GT sample and the 1Fe:5GT sample as almost identical scans. There is no discernable

peak in the two-theta region of 44.7°, where metallic iron presents its primary peak, nor any other peaks characteristic of iron oxides. The lack of observable peaks may be related to the very low amount of iron in the recovered solid, so it is not conclusive evidence for the absence of crystalline Fe minerals. Nadagouda et al. (2009) also reported similar XRD patterns of various mixtures of green tea with Fe^{3+} solution.

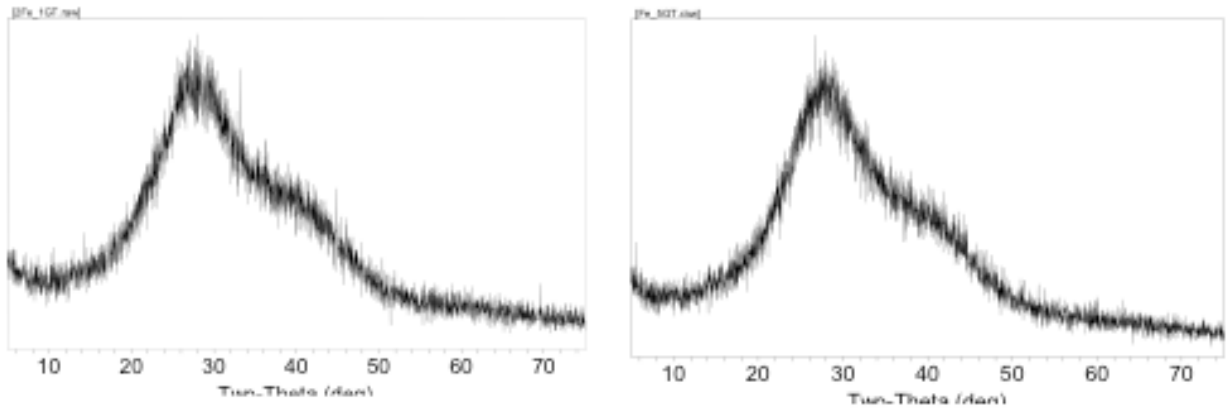

Figure 4.3.13 XRD scan of 2FE:1GT and 1Fe:5GT Samples

4.4 Hexavalent Chromium Reduction

The reductive capabilities of the three different mixing ratios were tested in the liquid fraction, solid fraction, and in the full suspension usingCr(VI) as the oxidant. The reductive capability of the filtered green tea alone was also tested and compared to previous data obtained for the unfiltered solution prepared with the same method (Harrigan and Szerakowski, 2013). The average results with standard deviation are shown in Table 4.4.1 and Figure 4.4.1. These are all based on 10mL of original suspension.

Table 4.4.1: Hexavalent Chromium Reduction by 10 mL offractionated and full suspensions

Sample ID	Fraction Tested	Cr(VI) Removed (mg)	Cr(VI) Removed by Fe^{2+}measured in Liquid Fraction (mg)	Cr(VI) removed by Green Tea* in Liquid Fraction (mg/mL)
2Fe:1GT	Liquid Fraction	1.03 ±0.02	0.69 ± 0.31	0.15
	Solid Fraction	8.00 ± 0.06	x	x
	Full Suspension	16.80		
1Fe:2GT	Liquid Fraction	0.96 ± 0.13	0.47 ± 0.26	0.15
	Solid Fraction	8.05 ± 1.12	x	x
	Full Suspension	15.26		
1Fe:5GT	Liquid Fraction	0.98 ± 0.15	0.35 ± 0.26	0.20
	Solid Fraction	7.56 ± 0.43	x	x
	Full Suspension	15.03		
Green Tea Only	Liquid Fraction	0.57	x	0.11
	Solid Fraction	6.38		X
	Full Solution**	7.10		0.71

***Assuming all Cr(VI) reduction that is not due to Fe^{2+}measured in the liquid fraction**
**** Data from Harrigan and Szerakowski (2013)**

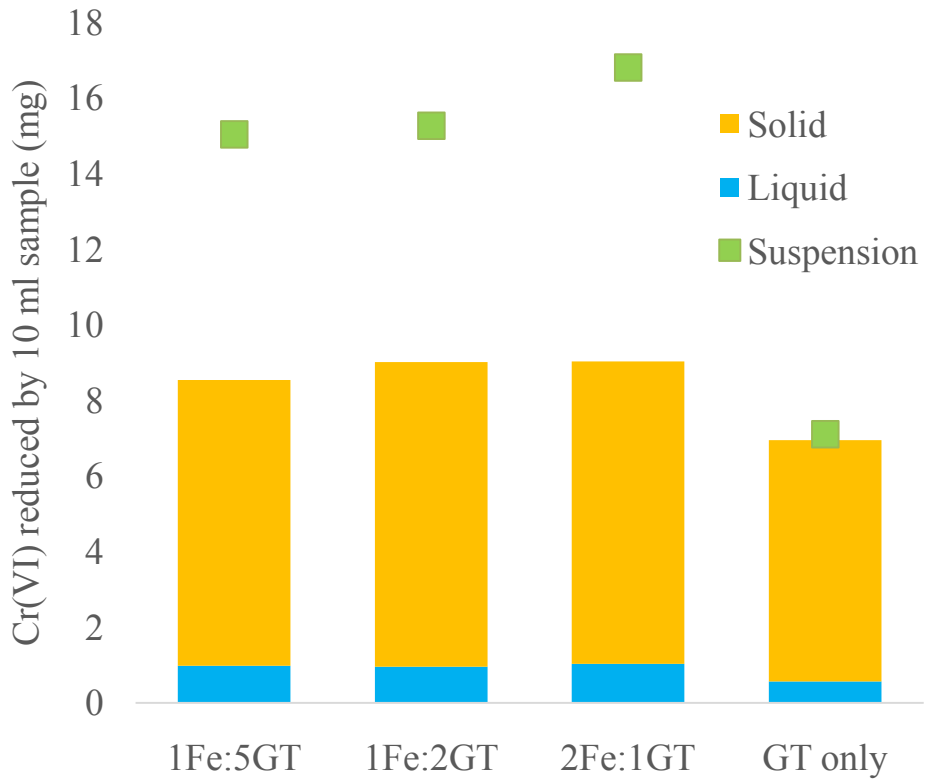

Figure 4.4.1: Average Cr(VI) reduction by 10 mL offractionated and full suspensions

The results indicate that there is perfect agreement between the amount of Cr(VI) reduced by the green tea solution alone both unfiltered and filtered. Nanofiltration involves the separation of large organic molecules and other compounds through mechanisms of size exclusion and adsorption. López-Muñoz et al. (2009) determined a molecular weight cut-off (MWCO) of 340 for the NF 270 membrane used in this study, which correspond to the MW weight of a compound retained with 90% efficiency by the membrane.Figure 4.4.2 shows the retention curve as a function of MW. This curve was developed using polyethylene glycol compounds, which are uncharged and should not exhibit significant adsorption (López-Muñoz et al. 2009). However, polyphenols should also be uncharged at pH 2, given that the pK_as of most polyphenols compounds are in the neutral-to-alkaline region. Thus, we will consider for simplicity that the retention of polyphenols approaches the curves developed for PEGs.

Comparing these values to the MW values of Table 2.2.1, it is apparent that the majority of the polyphenols should be retained by the membrane where only ~15% of EGC may pass through the membrane, and about 35-40% of caffeine and gallic acid. It is known that Cr(VI) can be reduced by caffeic acid that has similar structure (Deiana et al., 2007), so that it is very likely that caffeine and gallic acid are Cr(VI) reductants as well. Based on the retention curve and using the average molar fractions of Table 2.2.1, it follows that only 17% of the original mols of polyphenols are present in the liquid fraction. Table 5.4.1 indicates that the "liquid" fraction of green tea (i.e. the fraction that goes through the NF 270 membrane) possesses only 15% of the total reductive capacity of the original green tea solution. Thus, the two analyses are in good agreement.

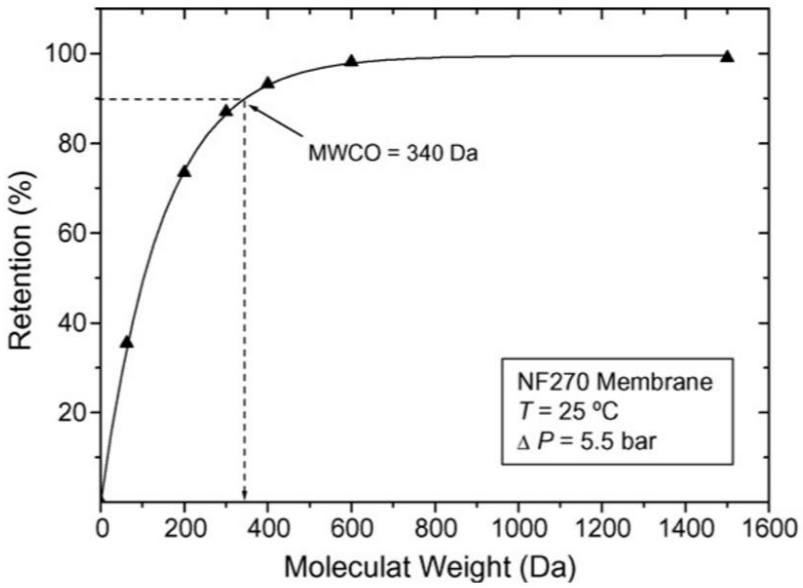

Figure 4.4.2: NF 270 retention curves for model polyethylene glycol compounds (López-Muñoz et al. 2009)

In contrast to green tea alone, there is poor agreement when comparing the reductive capacity of the GT-nZVI suspensions and the sum of the respective solid and liquid fractions. Specifically, the additive reductive capacity is 53-59% of the suspension reductive capacity for

all three formulations. The analysis of the green tea alone indicates that filtration does not affect the reductive capacity of the organic molecules. Thus, it is probable that the iron present on the filter loses its reductive capacity as a result of the filtration process. This loss may be due to several processes, such as oxidation and agglomeration. It is also possible that the continuous presence of green tea in solution may lead to regeneration of Fe(II) after reaction with Cr(VI), further enhancing the reaction, which cannot occur as easily in the solid phase. This result is important for the interpretation of the solid analyses, all of which rely on solids recovered from filtration, with the exception of XANES performed directly on the suspension.

Interestingly, there were very small differences in the performance of the three mixes. Notably, both the liquid and the solid had no statistically significant differences, while the 2Fe:1GT suspension had slightly higher reduction compared to the 1Fe:2GT and 1Fe:5GT (these are single values). There are several processes to decouple in order to explain these results, namely:

- The mass of initial polyphenols decreases with increasing Fe.
- The mass of polyphenols reacting with the added Fe(III) increases with increasing Fe. It is not trivial to assess the available concentration remaining in the GT-nZVI suspension that can further reduce either Cr(VI) or Fe(III) resulting from Cr(VI)-Fe(II) reaction.
- The mass and reactivity of polyphenols that are retained in the solid vs. pass in the liquid fraction are also likely different in the three mixes. One cannot assume that the organic molecules in the liquid of green tea alone are the same as in the liquid of the filtered GT-nZVI suspension.

Answering these questions requires more detailed investigation with regard to the reactions of specific polyphenols that are beyond the scope of this study.

5. Conclusions

The purpose of this research was to gain insight into the reductive actions of green tea polyphenols on ferric iron and to assess the claim that synthesis of zero-valent iron from this reaction is viable. The XANES analysis on the full suspensions has shown that zero-valent iron does not predominantly present itself from the simple mixing of green tea and ferric iron. It was qualitatively determined that a mixed Fe(II)-Fe(III) species is the predominant component of this suspension.

For all other experiments the solid fractions and the liquid fractions were separated and analyzed individually. The reduction experiments using hexavalent chromium showed that this separation reduces the overall reductive capacity, possibly due to oxidation of iron or due to elimination of iron regeneration by polyphenols. Therefore, there are limitations to this approach of separating the liquid and the solid to characterize the whole suspension. The reduction experiments also showed that both the solid and liquid fractions had reducing iron species present in all ratios and thatthe reductive capacity for Cr(VI) is not dramatically influenced by the change in the green tea:iron ratio. While the 2Fe:1GT suspension showed the highest overall reduction, it also had the highest percentage of Fe^{3+} in the liquid and had a higher initial Fe concentration. Therefore, it is suggested that the 1Fe:2GT suspension is most suitable for remediation.

The liquid fraction analysis showed that reduction efficiency of iron increased with increasing iron concentration. However, this also led to an excess of Fe^{3+} remaining in solution as the total polyphenol content was less.

The solid fraction analyses were performed in a complementary fashion to each other to determine the most likely components of the given mixtures. The Mössbauer solid analysis

showed that the interaction of polyphenols with iron produces organic complexes with a distinctive inhibition of oxide or hydroxide formation in the solidfraction of all mixtures, except at very high iron concentrations. Both ferrous iron and ferric iron were present in all mixtures, with the highest percentage correlating to the highest iron ratio in the 2Fe:1GT mixture. These findings were consistent with previous polyphenol-iron investigations that found reduction of ferric iron to ferrous iron. There was no evidence of zero-valent iron in any of the samples.

The XANES solid analysis showed that a mixture of Fe(II)-Fe(III) was the most likely predominant species, given the Mössbauer analysis precluding oxides and hydroxides. A specific compound was not verified as many standard spectra were not available. The XPS solid analysis showed a distinctive lack of zero-valent iron identification, but exact speciation was not possible using the spectra curves available. XRD analysis also showed no indication of zero-valent iron in any sample.

This research has shown that the interactions between polyphenols in tea and iron are extremely complex and create highly heterogeneous mixtures that are difficult to characterize and are likely to change under slightly varying conditions. In order to definitely characterize these mixtures, further study needs to be performed on individual polyphenol groups and species to determine their individual effect on reducing iron and their relative effect to each other in a solution as complex as tea. Further studies in organics-iron interactions would also be improved with increased access to standard spectra for these organic complexes. This work was limited by available spectra and by the assumptions made in regards to the polyphenol groups present in green tea. This work can conclude that the simple mixing of green tea and ferric iron does not predominantly produce stable zero-valent iron. The resulting iron is most likely represented in a mixed Fe(II)-Fe(III) organometallic compound.

References

C. Anesini, G. E. Ferraro, R. Filip. "Total Polyphenol Content and Antioxidant Capacity of Commercially Available Tea (Camellia sinensis) in Argentina." J. Agric. Food Chem. 56 (2008) pp. 9225-9229.

T. Bigg& S. J. Judd. "Zero-Valent Iron for Water Treatment." Environmental Technology. 21 (2000) pp. 661-670.

J. Blomquist, U. Helgeson, L. C. Moberg, B. Folkesson, R. Larsson.*Inorg*. *Chim*. *Acta* 69, 17 (1983)

M. D. Dyar, D. G. Agresti, M. W. Schaefer, C. A. Grant, E. C. Sklute. "Mössbauer Spectroscopy of Earth and Planetary Materials." *Annu*. *Rev*. *Earth Planet*. *Sci*. 34 (2006) pp. 83-125.

Z. Fang, X. Qiu, R. Huang, X. Qiu, M. Li. "Removal of chromium in electroplating wastewater by nanoscale zero-valent metal with synergistic effect of reduction and immobilization." Desalination. 280 (2011) pp. 224-231.

K. D. Grieger, A. Fjordboge, N. B. Hartmann, E. Eriksson, P. L. Bjerg, A. Baun. "Environmental benefits and risks of zero-valent iron nanoparticles (nZVI) for in situ remediation: Risk mitigation or trade-off?" J. Contaminant Hydrology. 118 (2010) pp. 165-183.

J. Gust, and J. Suwalski. "Use of Mössbauer Spectroscopy to Study Reaction Products of Polyphenols and Iron Compounds." *Corrosion Science*. 5 (1994) pp 355-365.

K. Harrigan and S. Szerakowksi. "Reduction of Hexavalent Chromium by Green Tea Polyphenols", Undergraduate Thesis, Environmental Engineering Program, University of Connecticut (2013).

S. M. Henning, C. Fajardo-Lira, H. W. Lee, A. A. Youssefian, V. L. W. Go, D. Heber. "Catechin Content of 18 Teas and a Green Tea Extract Supplement Correlates With the Antioxidant Capacity." Nutrition and Cancer. 45 (2003) pp. 226-235.

G. E. Hoag, J. B. Collins, J. L. Holcomb, J. R. Hoag, M. N. Nadagoua, R. S. Varma. "Degradation of bromothymol blue by 'greener' nano-scale zero-valent iron synthesized using tea polyphenols." J. Materials Chemistry. 19 (2009) pp. 8671-8677.

D. L. Huber. "Synthesis, Properties, and Applications of Iron Nanoparticles." Small, 1 (2005) pp. 482–501.

M. J. Hynes, and M. Ó. Coinceanainn. "The kinetics and mechanisms of the reaction of iron(III) with gallic acid, gallic acid methyl ester and catechin. J. Inorg. Biochem. 85 (2001) pp. 131-142.

J. A. Jaén, J. De Obaldía, M. V. Rodríguez. “Application of Mössbauer spectroscopy to the study of tannins inhibition or iron and steel corrosion.” *Hyperfine Interactions*. 202 (2011) pp. 25-38.

J. A. Jaén, E García de Saldaña, C. Hernández. “Characterization of reaction products of iron and iron salts and aqueous plant extracts.” *Hyperfine Interactions*. 122 (1999) pp. 139-145.

J. A. Jaén, L. González, A. Vargas, G. Olave. “Gallic Acid, Ellagic Acid and Pyrogallol Reaction with Metallic Iron. *Hyperfine Interactions*. 148 (2003) pp. 227-235.

J. A. Jaén, and C. Navarro. “Mössbauer and infrared spectroscopy as a diagnostic tool for the characterization of ferric tannates.” *Hyperfine Interactions* 192 (2009) pp. 61-67.

B. Kharisov, R. Dias, O. Kharissova, V. Jiménez-Pérez, B. Pérez, B. Flores. “Iron-containing nanomaterials: synthesis, properties, and environmental applications.” RSC Advances. 2 (20120) pp. 9325-9358.

X-Q. Li, D. W. Elliott, W-X. Zhang. “Zero-Valent Iron Nanoparticles for Abatement of Environmental Pollutants: Materials and Engineering Aspects.” Critical Reviews in Solid State and Materials Sciences. 31 (2006) pp. 111-122.

J.X. Liu, C. Wang, J.Y. Shi, H. Liu, Y.X. Tong. “Aqueous Cr(VI) reduction by electrodeposited zero-valent iron at neutral pH: acceleration by organic matters.” J. Hazard. Mater. 163 (2009) pp. 370-375.

B.A. Manning, J.R. Kiser, H. Kwon, S.R. Kanel. “Spectroscopic investigation of Cr(III)- and Cr(VI)- treated nanoscalezero-valent iron.” Environ. Sci. Technol. 41 (2007) pp. 586-592.

Material’s Data Inc. (MDI). (2008). Jade Version 8.5, California, U.S.A

A. Matlochová, D. Planchá, N. Rapantová. “The Application of Nanoscale Materials in Groundwater Remediation.” J. Env. Stud. 22 (2013) pp. 1401-1410.

R. I. Mellican. “The Interaction of Iron With Polyphenols.” ProQuest Dissertations and Theses. Purdue University. 2001.

N. C. Mueller, J. Braun, J. Bruns, M. Cernik, P. Rissing, D. Rickerby, B. Nowack. “Applications of nanoscale zero valent iron (NZVI) for groundwater remediation in Europe.” Environ. Sci. Pollut. Res. 19 (2012) pp. 550-558.

N. C. Müller, and B. Nowack. "Nano zero valent iron—The solution for water and soil remediation." Report of the ObservatoryNANO (2010) pp. 1-34.

M. N. Nadagouda, A. B. Castle, R. C. Murdock, S. M. Hussain, R. S. Varma. “In vitro biocompatibility of nanoscalezero-valent iron particles (NZVI) synthesized using tea polyphenols.” Green Chemistry. 12 (2010) pp. 114-122.

M. Otto, M. Floyd, S. BajPai. “Nanotechnology for site remediation.” Remediation. 19 (2008).

N. R. Perron, and J. L. Brumaghim. “A Review of the Antioxidant Mechanisms of Polyphenol Compounds Related to Iron Binding.” Cell BiochemBiophys. 53 (2009) pp. 75-100.

B. Ravel, and M. Newville. “ATHENA, ARTEMIS, HEPHAESTUS: data analysis for X-ray absorption spectroscopy using IFEFFIT.” J. Synchrotron Radiat.12 (2005) pp. 537–541.

P. Ryan, and M. J. Hynes. “The kinetics and mechanisms of the complex formation and antioxidant behavior of the polyphenols EGCg and ECG with iron (III).” J. Inorg. Biochem. 101 (2007) pp. 585-593.

S. Sivastava, S. Badrinarayanan, A. J. Mukhedkar.Polyhedron 4, 409 (1985).

Y-P. Sun, X-Q. Li, J. Cao, W-X. Zhang, H. P. Wang. “Characterization of zero-valent iron nanoparticles.” Advances in Colloid and Interface Science. 120 (2006) pp. 47-56.

F.E. Viteri, E. Alvarez, R. Batres. “Fortification of Sugar with NaFeEDTA improves Iron Status in Semirural Guatemalan Populations”. American Journal of Clinical Nutrition, 61 (1995) pp. 1153-1163.

R. Yuvakkumar, V. Elango, V. Rajendran, N. Kannan. “Preparation and Characterization of Zero Valent Iron Nanoparticles.” J. Nanomaterials and Biostructures. 6 (2011) pp. 1771-1776.

Appendix A: Mass Balance on Fe Filtration

					AA results	Assuming all 10 mL are recovered	Initial minus total out	Ferrozine	In the original V	Using FeII from ferrozine
GT:Fe	Cin (mM)	V (mL)	M in (mmol)	M in (mg)	Fe tot out (mM)	Fe tot out (mg)	Fe precipitated (mg)	Fe(II) outflow (mM)	Fe(II) outflow (mmol)	Cr(VI) reduction potential (mmol)
Test A										
5:1	17	5	0.085	4.75	0.95	0.27	4.48	0.76	0.0038	0.00127
2:1	33	5	0.165	9.21	2.17	0.61	8.61	1.62	0.0081	0.00270
1:2	66	5	0.33	18.43	3.31	0.92	17.50	1.41	0.00705	0.00235
GT only										0
Test B										
5:1	17	5	0.085	4.75	1.2	0.34	4.41	0.93	0.00465	0.00155
2:1	33	5	0.165	9.21	10.14	2.83	6.38	9.28	0.0464	0.01547
1:2	66	5	0.33	18.43	8.91	2.49	15.94	6.39	0.03195	0.01065
Test C										
5:1	17	5	0.085	4.75	1.9	0.53	4.22	1.45	0.00725	0.00242
2:1	33	5	0.165	9.21	8.33	2.33	6.89	7.52	0.0376	0.01253
1:2	66	5	0.33	18.43	12.02	3.36	15.07	7.38	0.0369	0.01230
Test D										
5:1	17	5	0.085	4.75	7.76	2.17	2.58	7.41	0.03705	0.01235
2:1	33	5	0.165	9.21	17.55	4.90	4.31	8.82	0.0441	0.01470
1:2	66	5	0.33	18.43	16.52	4.61	13.82	7.12	0.0356	0.01187
Test E										
5:1	17	5	0.085	4.75	3.14	0.88	3.87	1.95	0.00975	0.00325
2:1	33	5	0.165	9.21	5.07	1.42	7.80	3.38	0.0169	0.00563
1:2	66	5	0.33	18.43	16.29	4.55	13.88	4.93	0.02465	0.00822
Test F										
5:1	17	5	0.085	4.75	2.05	0.57	4.17	0.88	0.0044	0.00147
2:1	33	5	0.165	9.21	7.26	2.03	7.19	4.93	0.02465	0.00822
1:2	66	5	0.33	18.43	17.15	4.79	13.64	6.3	0.0315	0.01050

Mass Balance Continued	Cr reduction experimental conditions			Theoretical with FeII from Ferrozine		Actual				Theoretical Ferrozine minus actual		Assuming additional reduction came from GT
GT:Fe	Cr(VI) initial C (mg/L)	Cr(VI) initial V (mL)	Cr(VI) initial (mmol)	Cr(VI) final (mmol)	Cr(VI) final (mg/L)	Cr(VI) final (mg/L)	Cr(VI) mmol	Cr(VI) removed (mg)	Cr(VI) removed by Fe(II) (mg)	Additional Cr(VI) removed (mg)	Initial mL GT	Additional Cr(VI) removed mg /mL GT
Test A												
5:1	50	25.00	0.0240	0.0228	39.47	3.16	0.001823077	1.1552	0.065866667	1.09	4.17	0.2614
2:1	50	25.00	0.0240	0.0213	36.99	4.92	0.002838462	1.1024	0.1404	0.96	3.33	0.2886
1:2	50	25.00	0.0240	0.0217	37.59	7.45	0.004298077	1.0265	0.1222	0.90	1.67	0.5426
GT only	50	25.00	0.0240	0.0240	50.00	27.31	0.013129808	0.56725	0	0.57	5.00	0.11
Test B												
5:1	50	25.00	0.0240	0.0225	38.98	3.16	0.001823077	1.1552	0.0806	1.07	4.17	0.2579
2:1	50	25.00	0.0240	0.0086	14.86	4.92	0.002838462	1.1024	0.804266667	0.30	3.33	0.0894
1:2	50	25.00	0.0240	0.0134	23.21	7.45	0.004298077	1.0265	0.5538	0.47	1.67	0.2836
Test C												
5:1	50	25.00	0.0240	0.0216	37.48	3.16	0.001823077	1.1552	0.125666667	1.03	4.17	0.2471
2:1	50	25.00	0.0240	0.0115	19.94	4.92	0.002838462	1.1024	0.651733333	0.45	3.33	0.1352
1:2	50	25.00	0.0240	0.0117	20.35	7.45	0.004298077	1.0265	0.6396	0.39	1.67	0.2321
Test D												
5:1	50	25.00	0.0240	0.0117	20.26	3.16	0.001823077	1.1552	0.6422	0.51	4.17	0.1231
2:1	50	25.00	0.0240	0.0093	16.19	4.92	0.002838462	1.1024	0.7644	0.34	3.33	0.1014
1:2	50	25.00	0.0240	0.0122	21.10	7.45	0.004298077	1.0265	0.617066667	0.41	1.67	0.2457
Test E												
5:1	50	25.00	0.0240	0.0208	36.03	11.37	0.006559615	0.9089	0.169	0.74	4.17	0.1776
2:1	50	25.00	0.0240	0.0184	31.90	12.47	0.007194231	0.8759	0.292933333	0.58	3.33	0.1749
1:2	50	25.00	0.0240	0.0158	27.42	6.43	0.003709615	1.0571	0.427266667	0.63	1.67	0.3779
Test F												
5:1	50	25.00	0.0240	0.0194	33.66	12.42	0.007165385	0.8774	0.240066667	0.64	4.17	0.1530
2:1	50	25.00	0.0240	0.0172	29.82	11.84	0.006830769	0.8948	0.355333333	0.54	3.33	0.1618
1:2	50	25.00	0.0240	0.0042	7.23	8	0.004615385	1.01	1.033066667	-0.02	1.67	-0.0138

*** All values in red were determined to be outliers and not used in analysis**

Appendix B: Hexavalent Chromium Reduction Data

Solid data for 10mL of Suspension

Test D	Cr(VI) initial C (mg/L)	Cr(VI) initial V (mL)	Cr(VI) final C (mg/L)	Cr reduced (mg)	Total Mass (mg)	Total Fe mass (mg)	Initial suspension (mL)
1Fe:5GT	50	200	13.74	7.252	77.75	3.5092998	10
1Fe:2GT	50	200	13.7	7.26	82.75	5.3812242	10
2Fe:1GT	50	200	10.2	7.96	129.75	12.0558186	10
GT only	50	200	18.12	6.376	48.75		10
Test E							
2Fe:1GT	50	100	3.8	4.62			10
Test F							
1Fe:5GT	50	200	10.7	7.86			10
1Fe:2GT	50	200	5.77	8.846			10
2Fe:1GT	50	200	9.8	8.04			10

Suspension data for 5mL

Test G	Cr(VI) initial C (mg/L)	Cr(VI) initial V (mL)	Cr(VI) final C (mg/L)	Cr reduced (mg)	Initial suspension (mL)
1Fe:5GT	50	200	12.42	7.516	5
1Fe:2GT	50	200	11.84	7.632	5
2Fe:1GT	50	200	8.01	8.398	5

Hexavalent Chromium Reduction Data Continued

Liquid Data for 5 mL Solution				**Extrapolated to 10 mL solution**			Average		
Test D	Cr(VI) removed by liquid (mg)	Cr(VI) removed by Fe(II) in liquid (mg)	Additional Cr(VI) removed by liquid (mg)	Cr(VI) removed by liquid (mg)	Cr(VI) removed by Fe(II) in liquid (mg)	Additional Cr(VI) removed by liquid (mg)	Cr reduced by solid	Cr reduced liquid + solid	Cr reduced by suspension
1Fe:5GT	1.16	0.64	0.51	2.31	1.28	1.03	7.252	9.56	15.032
1Fe:2GT	1.10	0.76	0.34	2.20	1.53	0.68	7.26	9.46	15.264
2Fe:1GT	1.03	0.62	0.41	2.05	1.23	0.82	7.96	10.01	16.796
GT only	0.56725	0	0.57	1.13	0.00	1.13	6.376	7.51	-
Test E									
1Fe:5GT	0.9089	0.169	0.74	1.8178	0.338	1.4798	-	-	15.032
1Fe:2GT	0.8759	0.292933333	0.58	1.7518	0.585866667	1.165933333	-	-	15.264
2Fe:1GT	1.0571	0.427266667	0.63	2.1142	0.854533333	1.259666667	4.62	6.7342	16.796
Test F									
1Fe:5GT	0.88	0.240066667	0.64	1.75	0.48	1.27	7.86	9.61	15.032
1Fe:2GT	0.89	0.355333333	0.54	1.79	0.71	1.08	8.846	10.64	15.264
2Fe:1GT	1.01	1.033066667	-0.02	2.02	2.07	-0.05	8.04	10.06	16.796